Stabilization of Large Motions of Euler-Bernoulli Beams by Boundary Controls

K. D. Do

Department of Mechanical Engineering, Curtin University, Bentley, WA 6102, Australia
Email: duc@curtin.edu.au

This paper proposes a design of boundary controls for stabilization of Euler-Bernoulli beams with large motions and non-neglectable moment of inertia under external loads. Common types of boundary conditions in practice are considered. The designed boundary controllers guarantee globally practically $\mathcal{K}_\infty$-exponentially stability of the closed-loop system. The control design, well-posedness, and stability analysis are based on two Lyapunov-type theorems developed for a class of evolution systems in Hilbert space.

Keywords: Euler-Bernoulli beams; Large motion; Boundary control; Hilbert space; Evolution system.

1. Introduction

Euler-Bernoulli beams, whose dynamics are described by partial differential equations (PDEs) subject to certain boundary conditions, are used in various applications. Theoretically, solutions of PDEs depend on boundary conditions. Thus, a change of the boundary conditions in a proper way would result in desired solutions of the PDEs. Practically, controls being implemented at boundaries are much more practical than distributed controls. Motivated by the above facts, boundary control of Euler-Bernoulli beams has received extensive attention from researchers over the last few decades, see for example (Chen, Chentouf, & Wang, 2014; Chentouf & Wang, 2015; Do, 2017a, 2017b; Do & Pan, 2008a; Fard & Sagatun, 2001; B. Z. Guo, 2001; B. Z. Guo & Jin, 2013; F. Guo & Huang, 2001; Harland, Mace, & Jones, 2001; He, Huang, & Li, 2017; He, Nie, Meng, & Liu, 2017; Jin & Guo, 2015; Li, Xu, & Han, 2016; Liu & Liu, 1998, 2000; Lu, Chen, Yao, & Wang, 2013; Luo, Guo, & Morgul, 1999; Meurer, Thull, & Kugi, 2008; Miletíc, Stürzer, Arnold, & Kugi, 2016; Nguyen, Do, & Pan, 2013; Özer, 2017; Queiroz, Dawson, Nagarkatti, & Zhang, 2000) based on the Lyapunov direct and flatness methods and (Bohm, Krstic, Kuchler, & Sawodny, 2014; Krstic & Smyshlyaev, 2008; Paranjape, Chung, & Krstic, 2013) based on the backstepping method on single beams, and (Henikl, Kemmetmüller, Meurer, & Kugi, 2016; Kater & Meurer, 2016; Lagnese, Leugering, & Schmidt, 1994) on multiple beams. These works contributed excellent results on reducing vibration of the beams via boundary controls at one end and the other end is either connected to the base via a fixed or ball/simple joint or connected to a tip mass. The control design is usually based on Lyapunov's direct and backstepping methods. Well-posedness of the closed-loop system is often carried out by using the Galerkin approximation or abstract method. In the above works and many others not listed here, mathematical models used for boundary control were often obtained from either linearization or Maclaurin series expansions up to the second order of the strain and bending angle, see (Eringen, 1952; Love, 1920), and therefore can only describe small motions (i.e., displacements and velocities of both translations and rotations with very small amplitudes). These models cannot describe any large motions (i.e., large magnitude of displacements and velocities of both translations and rotations) because otherwise the linearized model is invalid.

Euler-Bernoulli beams are slender (say, the ratio of diameter to length is less than 10^{-2}) and extensible. They deform in the transverse and longitudinal directions instead of shearing that can occur for thick (Timoshenko) beams, see for example (Do, 2017c; Endo, Matsuno, & Jia, 2017; Queiroz et al., 2000). Therefore, Euler-Bernoulli beams are suffering from nonlinear and large motions induced by external loads. Boundary control of Euler-Bernoulli beams with large motions has received less attention. In (Do, 2011; Do & Pan, 2009a) (see also (Athisakul, Monprapussorn, & Chucheepsakul, 2011; Kokarakis & Bernitsas, 1987) for models of Euler-Bernoulli beams, where only large deflection is considered), boundary control of Euler-Bernoulli beams (risers) with large deflections was considered. In these works, the rotational inertia is neglected and one end of the beam is connected to the fixed base by a ball joint. Moreover, the beams are constrained to inextensibility.

In this paper, the problem of stabilization of Euler-Bernoulli beams subject to extensibility and non-neglectable rotary moment of inertia with large motions by boundary controls under external loads is addressed. Three common types of boundary conditions are considered. Of all these types, boundary controls forces are available only at the top-end. The lower-end is fixed to the base in Type I, and is connected to the based via ball/simple joint in Type II, see Figure 1.A. In Type III, the lower-end is connected to a payload, i.e., this end freely moves. Type I and Type II of boundary conditions are usually used in tension-legs and marine risers, respectively, while Type III is often met in sea and air transportatation/installation (such as gantry/overhead cranes). It will be seen in Section 4 that control design for Type III is much more challenging than that for Type I and Type II. Theoretically, Sobolev embedding has to be applied in an appropriate way to relate motions of the lower-end to the top-end. Moreover, the boundary controls need to propagate from the top-end to the lower-end through the beam body. Practically, it is not reasonable to implement an additional control at the lower-end due to hash environment.

Thus, this paper derives an appropriate nonlinear mathematical model that captures both large and vibrating motions of Euler-Bernoulli beams subject to extensibility and non-neglectable rotary moment of inertia. The beam dynamics are then transformed to a system of evolution equations described by a set of ordinary differential equations (ODEs) in Hilbert space for convenience of control design, well-posedness, and stability analysis. Next, two Lyapunov-type theorems are developed for study of well-posedness and stability analysis for a class of evolution systems. These theorems are then used to design boundary controllers that globally practically $\mathcal{K}_\infty$-exponentially stabilize the beam motions at the origin for all types of boundary conditions at the lower-end. The above approach has several significant advantages over conventional control design methods. First, various control design and stability analysis tools such as Lyapunov's direct method (Khalil, 2002) developed for ODEs in Euclidean space can be mimicked with appropriate functional spaces, norms and inner products introduced. Second, searching for a proper Lyapunov function can be constructive based on the backstepping method (Krstic, Kanellakopoulos, & Kokotovic, 1995). Third, well-posedness can be carried out for a class of systems governed by nonlinear PDEs, see (Banks, Smith, & Wang, 1996; Luo et al., 1999) for systems governed by linear PDEs, instead of considering each concrete system as in the conventional approach (e.g., (Berrimi & Messaoudi, 2004; Cavalcanti, Cavalcanti, & Soriano, 2002; Do, 2011, 2016a; Do & Pan, 2008a, 2009a; Evans, 2000)). In summary, the contributions of the present paper are listed as follows:

- Original nonlinear PDEs governing motions of Euler-Bernoulli beams are considered.
- Three common types of boundary conditions are addressed.
- Two Lyapunov-type theorems are developed to study well-posedness and ($\mathcal{K}_\infty$-exponential) stability of nonlinear evolution systems in Hilbert space.
- Boundary controllers are designed to achieve global well-posedness and $\mathcal{K}_\infty$-exponential stability of the closed-loop system under both low and high constant axial force (pretension).

Notations. The symbols $\wedge$ and $\vee$ denote the infimum and supremum operators, respectively. These operators are also applied to more than two arguments.

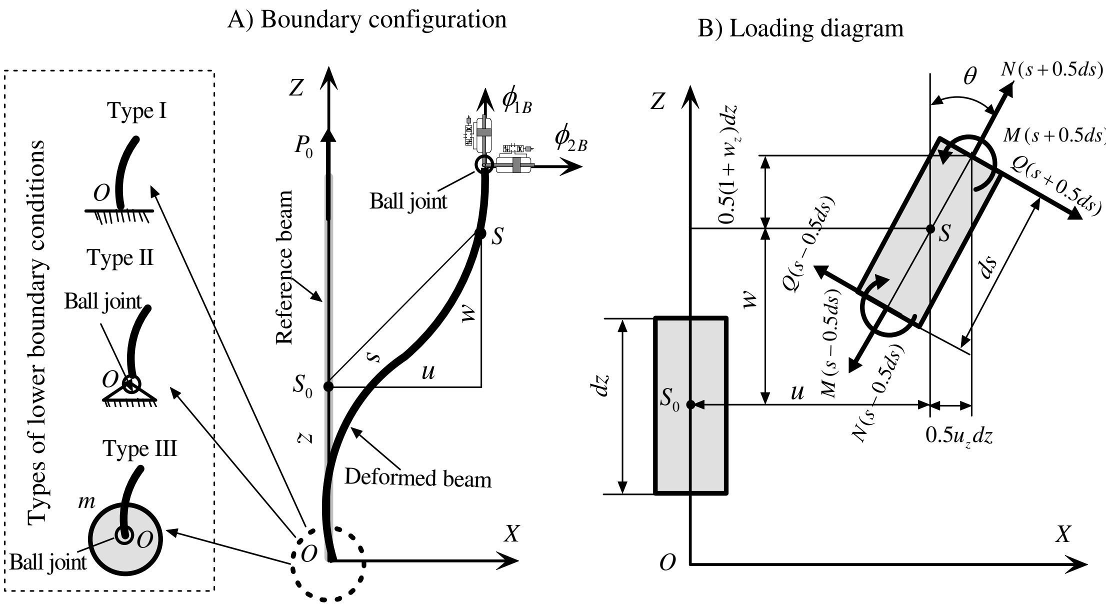

Figure 1.: A) Beam boundary configuration (ϕ_{1B} and ϕ_{2B} are boundary control forces provided by actuators); B) loading diagram.

2. Problem formulation

2.1. *Mathematical model*

Assume that the plane sections of the beam remain plane after deformation; the beam is locally stiff; the beam material is homogeneous and isotropic; torsional moment is neglected; only in-plane deformations of the beam occur; and the reference beam is straight. The beam's boundary configuration is shown in Fig. 1A and the loading diagram on an element is given in Fig. 1B, where the argument t and nonconservative forces are not shown for clarity; and all symbols are defined in the sequel. Let (u, w) denote the displacements of the beam along the OX- and OZ-axis from the point S_0 of the initial beam center line at the initial time t_0 to the point S of the deformed beam center line at time t, and θ denote the angle between the beam's center line and OZ-axis at the point S.

Balancing the forces and moments acting on the beam element results in the following equations of motion (Lacarbonara, 2013):

$$\begin{aligned} m_0 w_{tt} &= [N\cos(\theta) - Q\sin(\theta)]_z + f_1, \\ m_0 u_{tt} &= [N\sin(\theta) + Q\cos(\theta)]_z + f_2, \\ J_0\theta_{tt} &= M_z + (1+\varepsilon)Q + f_3, \end{aligned} \tag{1}$$

for all $(z, t) \in (0, \Gamma) \times [t_0, \infty)$ with Γ being the beam length at the reference state and $t_0 \geq 0$ being the initial time. In (1), where m_0 and J_0 are the mass and moment of inertia per unit length, respectively; the symbols $\bullet_t$ and $\bullet_z$ denote $\frac{\partial \bullet}{\partial t}$ and $\frac{\partial \bullet}{\partial z}$, respectively; $f_i(\bullet), i = 1, 2, 3$ denote nonconservative forces and moment; $N(z, t)$ and $Q(z, t)$ denote axial and shear forces, respectively; and $M(z, t)$ denotes the bending moment; $\varepsilon(z, t)$ denote the axial strain of the beam's center line. The axial strain and unshearable condition (as we are considering Euler-Bernoulli beams) are expressed in terms of $u_z(z, t)$, $w_z(z, t)$ and $\theta(z, t)$ as follows:

$$\begin{aligned} \varepsilon &= (1 + w_z)\cos(\theta) + u_z\sin(\theta) - 1, \\ 0 &= -(1 + w_z)\sin(\theta) + u_z\cos(\theta), \end{aligned} \tag{2}$$

for all $(z, t) \in [0, \Gamma] \times [t_0, \infty)$. We need to supply constitutive equations for $N(z, t)$ and $M(z, t)$. Because 1) the curvature and extensibility can be moderately large, 2) the selected base curve is the centroidal curve, and 3) the section-fixed axes are collinear with the principal axes of inertia and the origin is the center of mass, then the constitutive equations can be given by (Love, 1920):

$$N = EA\varepsilon + P_0, \;\; M = EI\theta_z, \tag{3}$$

for all $(z, t) \in [0, \Gamma] \times [t_0, \infty)$, where A is the cross section area; E is Young's modulus; I is the area moment of inertia of the beam cross section; and P_0 is the positive constant axial force. There is no constitutive equation for Q since it needs to satisfy the third equation of (1) and θ satisfies the second equation of (2), see also Remark 1 below. The forces and moment $f_i(\bullet), i = 1, 2, 3$ are given by:

$$f_1 = -d_1 w_t + d_{1K} w_{zzt} + f_{10}(z, t), \;\; f_2 = -d_2 w_t + d_{2K} u_{zzt} + f_{20}(z, t), \;\; f_3 = -d_3\theta_t + f_{30}(z, t), \tag{4}$$

where the positive constants $d_i, i = 1, 2, 3$ denote damping coefficients; the positive constants $d_{iK}, i = 1, 2$ are Kelvin-Voigt type damping coefficients; and $f_{i0}(z, t), i = 1, 2, 3$ denote the external loads. Note that the terms $d_{1K} w_{zzt}$ and $d_{2K} u_{zzt}$ are referred to as Kelvin-Voigt type damping terms (Meirovitch, 1967). The initial values are:

$$u(z, t_0) = u_{10}(z), u_t(z, t_0) = u_{20}(z), w(z, t_0) = w_{10}(z), w_t(z, t_0) = w_{20}(z). \tag{5}$$

Finally, referring to Fig. 1A the boundary conditions at the top-end are given as follows:

$$\begin{aligned} & m_{1B}w_{tt}(\Gamma,t) = -[N(\Gamma,t)\cos(\theta(\Gamma,t)) - Q(\Gamma,t)\cos(\theta(\Gamma,t)) - P_0] + \phi_{1B} - d_{1B}w_t(\Gamma,t) \\ & \qquad -d_{1K}w_{zt}(\Gamma,t) + f_{1B0}(t), \\ & m_{2B}u_{tt}(\Gamma,t) = -[N(\Gamma,t)\sin(\theta(\Gamma,t)) + Q(\Gamma,t)\cos(\theta(\Gamma,t))] + \phi_{2B} - d_{2B}w_t(\Gamma,t) \\ & \qquad -d_{2K}u_{zt}(\Gamma,t) + f_{2B0}(t), \\ & M(\Gamma,t) = 0, \end{aligned} \tag{6}$$

where the boundary control forces ϕ_{1B} (along the OZ-axis) and ϕ_{2B} (along the OX-axis) are provided by actuators; $m_{iB}, i = 1,2$ are masses of the actuators; the positive constants $d_{iB}, i = 1,2$ are damping coefficients; and $f_{iB0}(t), i = 1,2$ being external forces and moment acting on the actuators. The boundary conditions at the lower-end are given by

$$\begin{aligned} &\text{Type I:}\left\{ w(0,t) = 0,\ u(0,t) = 0,\ \theta(0,t) = 0. \right. \\ &\text{Type II:}\left\{ M(0,t) = 0,\ w(0,t) = 0,\ u(0,t) = 0. \right. \\ &\text{Type III:}\begin{cases} m_P w_{tt}(0,t) = -d_{1P}(t)w_t(0,t) + [N(0,t)\cos(\theta(0,t)) - Q(0,t)\cos(\theta(0,t)) - P_0] \\ \qquad +d_{1K}w_{zt}(0,t) + f_{1P0}(t), \\ m_P u_{tt}(0,t) = -d_{2P}(t)u_t(0,t) + [N(0,t)\sin(\theta(0,t)) + Q(0,t)\cos(\theta(0,t))] \\ \qquad +d_{2K}u_{zt}(0,t) + f_{2P0}(t), \\ M(0,t) = 0, \end{cases} \end{aligned} \tag{7}$$

where m_P is the mass of the payload; the positive constants $d_{iP}, i = 1,2$ are damping coefficients; and $f_{iP0}(t), i = 1,2$ are external forces and moment acting on the pay load. Note that for Type III, $P_0 = m_P g$, where g is the gravity acceleration.

Remark 1: *The shear force Q is obtained by solving the third equation of (1). Apparently, the force Q depends on θ_{tt}, which in turn depends on w_{ztt} and u_{ztt} because $\theta = \arctan\left(\frac{u_z}{1+w_z}\right)$, see the second equation of (2). Due to this dependence, we do not substitute the shear force Q, which is obtained by solving the third equation of (1), into the first two equations of (1), (6), and (7) because this substitution will result in a very complicated presentation of the beam dynamics and control design. Moreover, linearization of the beam dynamics (1)-(7) results in models studied in vibration works in Section 1, see (S. T. Chow & Sethna, 1965).*

Several useful inequalities to be used extensively in the control design and stability analysis later are given in the following lemma.

Lemma 2.1: *For all $(z,t) \in [0,\Gamma] \times [t_0,\infty)$, the following inequalities and equality hold:*

$$\begin{aligned} & \varepsilon(z,t) - w_z(z,t) \geq 0,\ \varepsilon^2(z,t) = w_z^2(z,t) + u_z^2(z,t) - 2(\varepsilon(z,t) - w_z(z,t)), \\ & \int_0^\Gamma w^2(z,t)dz \leq 2\Gamma w^2(\Gamma,t) + 4\Gamma^2\int_0^\Gamma w_z^2(z,t)dz,\ w^2(0,t) \leq 2w^2(\Gamma,t) + 4\Gamma\int_0^\Gamma w_z^2(z,t)dz. \end{aligned} \tag{8}$$

Proof. See Appendix A. The last two inequalities also hold for $w(z,t)$ being substituted by $u(z,t)$.

2.2. *Control objectives*

Before stating the control objective, we make the following assumption, which is reasonable in practice.

Assumption 2.1:

1) The initial values $u_{10}(z), u_{20}(z), w_{10}(z), w_{20}(z), \theta_{20}(z)$ are bounded in L^2-norm, i.e., there exists a nonnegative constant ϵ_0 such that $\int_0^\Gamma (u_{10}^2(z) + w_{10}^2(z) + u_{20}^2(z) + w_{20}^2(z) + \theta_{20}^2(z))dz \leq \epsilon_0$.

2) The external loads $f_{i0}(z,t)$, $f_{iB0}(t), i = 1,2,3,$ and $f_{iP0}, i = 1,2$ are bounded in the sense that there exist nonnegative constants f_{i0}^M, f_{iB0}^M, and f_{iP}^M such that

$$\sup_{t\in[t_0,\infty)} \int_0^\Gamma f_{i0}^2(z,t)dz \leq f_{i0}^M,\ \sup_{t\in[t_0,\infty)} f_{iB0}^2(t) \leq f_{iB0}^M,\ \sup_{t\in[t_0,\infty)} f_{iP0}^2(t) \leq f_{iP0}^M. \tag{9}$$

3) There exist constants ε_m and ε_M such that the axial strain $\varepsilon(z,t)$ satisfies $\varepsilon(z,t) \in [\varepsilon_m, \varepsilon_M]$

for all $(z,t) \in [0,\Gamma] \times [t_0,\infty)$ with $1+\varepsilon_m$ being strictly positive. This condition is practical because otherwise Hooke's law will not be applicable (Love, 1920).

4) The beam stiffness is not too small in the sense that

$$EA \gg \frac{d_{1K} \vee d_{2K}}{2} + 2\Gamma^2(d_1 \vee d_2), \tag{10}$$

where the symbol $\gg$ means strictly larger than. This condition makes sense because otherwise the beam will behave like a string/cable.

Control Objective 2.1: *Under Assumption 2.1, design the boundary controls $\phi_{iB}, i=1,2$ and the positive constant axial force P_0 such that the beam system consisting of (1)-(7) is globally (practically) $\mathcal{K}_\infty$-exponentially stable at the origin in the sense that*

$$\mathcal{E}(t) \leq \alpha(\mathcal{E}(t_0))e^{-c(t-t_0)} + c_0, \tag{11}$$

where α is a class $\mathcal{K}_\infty$-function, c is a positive constant depending on the initial conditions, c_0 is zero if $f_{i0}(\bullet)=0$, $f_{i0}(\bullet)=0$, $f_{iB0}(t)=0$, and $f_{iP0}(t)=0$ with $i=1,2,3$, and is a positive constant if $f_{i0}(\bullet)$, $f_{iB0}(t)$, and $f_{iP0}(t)$ satisfy (9); and $\mathcal{E}(t) := \mathcal{E}^{I,II}(t)$ for Types I and II, and $\mathcal{E}(t) := \mathcal{E}^{III}(t)$ with

$$\begin{aligned} &\text{Types I and II:} \left\{ \mathcal{E}^{I,II}(t) = \mathcal{E}^{\diamond}(t) + \mathcal{E}_0^{I,II}(t), \right. \\ &\text{Type III:} \left\{ \mathcal{E}^{III}(t) = \mathcal{E}^{\diamond}(t) + \mathcal{E}_0^{III}(t), \right. \end{aligned} \tag{12}$$

where $\mathcal{E}_0(t)$ depends on the type of boundary conditions at the lower-end as follows

$$\begin{aligned} \mathcal{E}^{\diamond}(t) &= \int_0^\Gamma \left[u_t^2(z,t) + w_t^2(z,t) + \theta_t^2(z,t) + \varepsilon^2(z,t) + \theta_z^2(z,t) \right] dz + \left[w_t(\Gamma,t) + \gamma w(\Gamma,t) \right]^2 \\ &\quad + \left[u_t(\Gamma,t) + \gamma u(\Gamma,t) \right]^2 + w^2(\Gamma,t) + u^2(\Gamma,t), \\ \mathcal{E}_0^{I,II}(t) &= 0, \ \mathcal{E}_0^{III}(t) = \left[w_t(0,t) + \gamma w(0,t) \right]^2 + \left[u_t(0,t) + \gamma u(0,t) \right]^2 + w^2(0,t) + u^2(0,t), \end{aligned} \tag{13}$$

with γ being a positive constant (to be chosen later). The matric $\mathcal{E}(t)$ is a positive definite and radially unbounded functional of velocities, displacements, and curvature of the whole beam body, and displacements of the both ends of the beam due to the Sobolev embedding (Adams & Fournier, 2003).

3. Well-posedness and Stability of Nonlinear Evolution Systems

3.1. *Space notations*

Let H be a separable Hilbert space identified with its dual H^* by the Riesz isomorphism. Let V be a real reflexible Banach space such that $V \subset H$ continuously and densely. Then for its dual space V^*, it follows that $H^* \subset V^*$. From the definitions of H and V, we have that the embedding $V \subset H \equiv H^* \subset V^*$ is continuous and dense. We denote by $\|.\|_H$, $\|.\|_V$, and $\|.\|_{V^*}$ the norms in H, V, and V^*, respectively; by $\langle .,. \rangle_{V,V^*}$ (i.e., $\langle \boldsymbol{z}, \boldsymbol{v} \rangle_{V,V^*} = \boldsymbol{z}(\boldsymbol{v})$ for $\boldsymbol{z} \in V^*, \boldsymbol{v} \in V$) the duality product between V and V^*; and by $\langle .,. \rangle_H$ the inner product in H. The duality product between V and V^* has the following property, see (Banks et al., 1996; Gawarecki & Mandrekar, 2011): $\langle \boldsymbol{u}, \boldsymbol{v} \rangle_{V,V^*} = \langle \boldsymbol{u}, \boldsymbol{v} \rangle_H, \boldsymbol{u} \in H, \boldsymbol{v} \in V$.

3.2. *Nonlinear Evolution systems*

On the space H, let us consider the nonlinear evolution system:

$$\frac{d\boldsymbol{X}(t)}{dt} = \boldsymbol{F}(\boldsymbol{X}(t),t), \ \boldsymbol{X}(t_0) = \boldsymbol{X}_0 \in H, \tag{14}$$

where $\boldsymbol{X} \in H$ and $\boldsymbol{F} : H \times [t_0,\infty) \to V^*$ is a family of nonlinear operators defined almost every (a.e.) t. We first define a variational solution of (14). This definition is a deterministic version of the one defined in (P. L. Chow, 2007).

Definition 1: *A H-valued process $\{\boldsymbol{X}(t), t \in [t_0, \infty)\}$ is said to be a global variational solution of (14) if for any $\boldsymbol{\psi} \in V$:*

$$\langle \boldsymbol{X}(t), \boldsymbol{\psi} \rangle_H = \langle \boldsymbol{X}_0, \boldsymbol{\psi} \rangle_H + \int_{t_0}^{t} \langle \boldsymbol{F}(\boldsymbol{X}(s), s), \boldsymbol{\psi} \rangle_{V,V^*} ds \tag{15}$$

for each $t \in [t_0, \infty)$.

The following stability definition is a version of the one in (Khalil, 2002) extended to Hilbert space.

Definition 2: *Let α be a class $\mathcal{K}_\infty$-function. The variational solution of (14) is said to be*
1) globally stable if, for each $\boldsymbol{X}_0 \in H$, there exists $\delta = \delta(\|\boldsymbol{X}_0\|_H)$ such that $\|\boldsymbol{X}(t)\|_H \leq \delta(\|\boldsymbol{X}_0\|_H)$, a.e. $(\boldsymbol{X}, t) \in V \times [t_0, \infty)$;
2) globally practically $\mathcal{K}_\infty$-exponentially stable if it is globally stable and $\|\boldsymbol{X}(t)\|_H \leq \alpha(\|\boldsymbol{X}(t_0)\|_H) e^{-c(t-t_0)} + c_0$, a.e. $(\boldsymbol{X}, t) \in V \times [t_0, \infty)$, where c is a positive constant depending on the initial conditions, and c_0 is positive constant. If $c_0 = 0$, it is globally $\mathcal{K}_\infty$-exponentially stable.

3.3. *Well-posedness and stability theorems for nonlinear evolution systems*

We assume that $\boldsymbol{F} : H \times [t_0, \infty) \to V^*$ is measurable and satisfies the following continuity and local monotonicity conditions.

Assumption 3.1:
1) [Continuity] The mapping $V \ni \boldsymbol{v} \mapsto \boldsymbol{F}(\boldsymbol{v}, t) \in V^*$ is continuous a.e. $t \in [t_0, \infty)$.
2) [Local monotonicity] For any $\boldsymbol{u}, \boldsymbol{v} \in V$ with $\|\boldsymbol{u}\|_H \leq \epsilon$ and $\|\boldsymbol{v}\|_H \leq \epsilon$, where ϵ is a positive constant, there exists a constant c_ϵ such that

$$2\langle \boldsymbol{u} - \boldsymbol{v}, \boldsymbol{F}(\boldsymbol{u}, t) - \boldsymbol{F}(\boldsymbol{v}, t) \rangle_{V,V^*} \leq c_\epsilon \|\boldsymbol{u} - \boldsymbol{v}\|_H^2, \tag{16}$$

a.e. $t \in [t_0, \infty)$.

Theorem 3.1: *Under Assumption 3.1, suppose that there exist a function $U \in C^1(H; [t_0, \infty))$ referred to as a Lyapunov function, and class $\mathcal{K}_\infty$-functions α_1 and α_2 such that*

$$\alpha_1(\|\boldsymbol{X}\|_H) \leq U(\boldsymbol{X}, t) \leq \alpha_2(\|\boldsymbol{X}\|_H), \text{ a.e. } (\boldsymbol{X}, t) \in V \times [t_0, \infty), \tag{17}$$

and that the generator $\mathcal{L}U := \frac{dU}{dt}$ given by

$$\mathcal{L}U(\boldsymbol{X}, t) = U_t(\boldsymbol{X}, t) + \langle \boldsymbol{F}(\boldsymbol{X}, t), U_{\boldsymbol{X}}(\boldsymbol{X}, t) \rangle_{V,V^*}, \tag{18}$$

with $U_t(\boldsymbol{X}, t)$ and $U_{\boldsymbol{X}}(\boldsymbol{X}, t)$ being the (Fréchet) derivatives of $U(\boldsymbol{X}, t)$ with respect to t and $\boldsymbol{X}$, respectively, satisfies

$$\mathcal{L}U(\boldsymbol{X}, t) \leq c(1 + U(\boldsymbol{X}, t)), \text{ a.e. } (\boldsymbol{X}, t) \in V \times [t_0, \infty), \tag{19}$$

where c is a nonnegative constant. Then (14) has a unique global variational solution for each $\boldsymbol{X}_0 \in H$.

Proof. The proof can be carried out by using the method of proving Theorem 4.1 in (Do, 2016b) and Theorem 4.1 in (Gawarecki & Mandrekar, 2011) (pages 176-181) with a note that only deterministic part is considered and that the coercivity condition is substituted by the condition (19).

Theorem 3.2: *Under Assumption 3.1, suppose that there exist a function $U \in C^1(H; [t_0, \infty))$ and a class $\mathcal{K}_\infty$-function α_2 such that*

$$c_1 \|\boldsymbol{X}\|_H^2 \leq U(\boldsymbol{X}, t) \leq \alpha_2(\|\boldsymbol{X}\|_H^2), \text{ a.e. } (\boldsymbol{X}, t) \in V \times [t_0, \infty), \tag{20}$$

where c_1 is a positive constant, and that

$$\mathcal{L}U(\boldsymbol{X}, t) \leq -c_3 \|\boldsymbol{X}\|_H^2 + c_0, \text{ a.e. } (\boldsymbol{X}, t) \in V \times [t_0, \infty), \tag{21}$$

where c_3 is a positive constant. If $c_0 = 0$, the equilibrium $\boldsymbol{X} \equiv 0$ is globally $\mathcal{K}_\infty$-exponentially stable. If c_0 is a positive constant, the equilibrium $\boldsymbol{X} \equiv 0$ is globally practically $\mathcal{K}_\infty$-exponentially stable.

Proof. See Appendix B.

4. Control design

4.1. *Abstract formulation*

Let $L^2(\mathcal{D})$ denote the L^2-space with the norm $\|.\|_{L^2}$ and inner product $\langle .,.\rangle_{L^2}$ and $W^{m,p}(\mathcal{D})$, with (m, p) being integers, denote the Sobolev space of order m and degree p, see (Adams & Fournier, 2003). Considering $z \in [0, \Gamma]$ as the parameter defined at every $t \geq t_0$, we can regard $u(z,t), w(z,t), \theta(z,t), u_t(z,t)$, $w_t(z,t)$, and $\theta_t(z,t)$ as $u_1(t) \in W^{2,2}([0,\Gamma])$, $w_1(t) \in W^{2,2}([0,\Gamma])$, $\theta_1(t) \in W^{2,2}([0,\Gamma])$, $u_2(t) \in L^2([0,\Gamma])$, $w_2(t) \in L^2([0,\Gamma])$, and $\theta_2(t) \in L^2([0,\Gamma])$, respectively. Similarly, $u(0,t), w(0,t), \theta_z(0,t)$, $u(\Gamma,t)$, $w(\Gamma,t)$, $\theta(\Gamma,t)$, $\theta_z(\Gamma,t)$ are regarded as $u_1^{B0}(t) \in \mathbb{R}$, $w_1^{B0}(t) \in \mathbb{R}$, $\mathbb{D}\theta_1^{B0}(t) \in \mathbb{R}$, $u_1^{B\Gamma}(t) \in \mathbb{R}$, $w_1^{B\Gamma}(t) \in \mathbb{R}$, $\theta_1^{B\Gamma}(t) \in \mathbb{R}$, $\mathbb{D}\theta_1^{B\Gamma}(t) \in \mathbb{R}$ respectively. Moreover, $u_t(\Gamma,t), w_t(\Gamma,t)$ and $\theta_t(\Gamma,t)$ are considered as $u_2^{B\Gamma}(t) \in \mathbb{R}, w_2^{B\Gamma}(t) \in \mathbb{R}$, and $\theta_2^{B\Gamma}(t)$, respectively. Let us also denote the operator $\mathbb{D}\phi(z) := \frac{\partial \phi}{\partial z}$. With the above notations, we can write the beam dynamics (1) and its boundary conditions (6) and (7) in the evolution system (abstract form):

$$\begin{aligned}
&\frac{dw_1}{dt} = w_2, \quad \frac{du_1}{dt} = u_2, \quad \frac{d\theta_1}{dt} = \theta_2 \\
&\frac{dw_2}{dt} = \frac{1}{m_0}\mathbb{D}[N\cos(\theta_1) - Q\sin(\theta_1)] + \frac{1}{m_0}f_1 := F_1, \\
&\frac{du_2}{dt} = \frac{1}{m_0}\mathbb{D}[N\sin(\theta_1) + Q\cos(\theta_1)] + \frac{1}{m_0}f_2 := F_2, \\
&\frac{d\theta_2}{dt} = \frac{1}{J_0}\Big[\mathbb{D}M + (1+\varepsilon)Q + f_3\Big] := F_3,
\end{aligned} \tag{22}$$

where the argument t is dropped for clarity. The boundary conditions (6) are written as:

$$\begin{aligned}
&\frac{dw_1^{B\Gamma}}{dt} = w_2^{B\Gamma}, \ \frac{du_1^{B\Gamma}}{dt} = u_2^{B\Gamma}, \\
&\frac{dw_2^{B\Gamma}}{dt} = \frac{1}{m_{1B}}\Big[-[N^{B\Gamma}\cos(\theta_1^{B\Gamma}) - Q^{B\Gamma}\sin(\theta_1^{B\Gamma}) - P_0] + \phi_{1B} - d_{1B}w_2^{B\Gamma} - d_{1K}\mathbb{D}w_2^{B\Gamma} + f_{1B0}\Big] := F_1^{B\Gamma}, \\
&\frac{du_2^{B\Gamma}}{dt} = \frac{1}{m_{2B}}\Big[-[N^{B\Gamma}\sin(\theta_1^{B\Gamma}) + Q^{B\Gamma}\cos(\theta_1^{B\Gamma})] + \phi_{2B} - d_{2B}u^{B\Gamma} - d_{2K}\mathbb{D}u_2^{B\Gamma} + f_{2B0}\Big] := F_2^{B\Gamma}, \\
&M^{B\Gamma} = 0,
\end{aligned} \tag{23}$$

where $N^{B\Gamma}(t)$, $Q^{B\Gamma}(t)$, and $M^{B\Gamma}(t)$ are the values of $N(t)$, $Q(t)$, and $M(t)$ evaluated at $z = \Gamma$, respectively, and the boundary conditions (7) are written in the abstract form as:

$$\begin{aligned}
&\text{Type I:} \big\{ w_1^{B0} = 0, \ u_1^{B0} = 0, \ \theta_1^{B0} = 0. \\
&\text{Type II:} \big\{ M^{B0} = 0, \ w_1^{B0} = 0, \ u_1^{B0} = 0. \\
&\text{Type III:} \begin{cases}
\dfrac{dw_1^{B0}}{dt} = w_2^{B0}, \ \dfrac{du_1^{B0}}{dt} = u_2^{B0}, \\
\dfrac{dw_2^{B0}}{dt} = \dfrac{1}{m_P}\Big[-d_{1P}w_2^{B0} + [N^{B0}\cos(\theta_1^{B0}) - Q^{B0}\cos(\theta_1^{B0}) - P_0] + d_{1K}\mathbb{D}w_2^{B0} + f_{1P0}\Big] := F_1^{B0}, \\
\dfrac{du_2^{B0}}{dt} = \dfrac{1}{m_P}\Big[-d_{2P}u_2^{B0} + [N^{B0}\sin(\theta_1^{B0}) + Q^{B0}\cos(\theta_1^{B0})] + d_{2K}\mathbb{D}u_2^{B0} + f_{2P0}\Big] := F_2^{B0}, \\
M^{B0} = 0,
\end{cases}
\end{aligned} \tag{24}$$

where $N^{B0}(t)$, $Q^{B0}(t)$, and $M^{B0}(t)$ are the values of $N(t)$, $Q(t)$, and $M(t)$ evaluated at $z = 0$, respectively.

4.2. *Control design*

To design the boundary controls $\phi_{iB}, i = 1, 2$, we consider the following Lyapunov functional candidate:

$$\begin{aligned}&\text{Types I and II}: \{U = U_1 + U_2 + U_3 + U_4^{\mathrm{I,II}},\\ &\text{Type III}: \{U = U_1 + U_2 + U_3 + U_4^{\mathrm{III}},\end{aligned} \tag{25}$$

where

$$\begin{aligned}
U_1 &= \frac{m_0}{2}\left[\|u_2\|_{L^2}^2 + \|w_2\|_{L^2}^2\right] + \frac{J_0}{2}\|\theta_2\|_{L^2}^2 + \frac{EA}{2}\|\varepsilon\|_{L^2}^2 + \frac{EI}{2}\|\mathbb{D}\theta_1\|_{L^2}^2 + P_0\langle 1, \varepsilon - \mathbb{D}w_1\rangle_{L^2},\\
U_2 &= \gamma m_0\langle w_1, w_2\rangle_{L^2} + \gamma m_0\langle u_1, u_2\rangle_{L^2} + \gamma J_0\left\langle \theta_2, \frac{\sin(\theta_1)}{1+\varepsilon}\right\rangle_{L^2},\\
U_3 &= \frac{m_{1B}}{2}\left[w_2^{B\Gamma} + \gamma w_1^{B\Gamma}\right]^2 + \frac{m_{2B}}{2}\left[u_2^{B\Gamma} + \gamma u_1^{B\Gamma}\right]^2 + k_{1B}\gamma(w_1^{B\Gamma})^2 + k_{2B}\gamma(u_1^{B\Gamma})^2,\\
U_4^{\mathrm{I,II}} &= 0,\\
U_4^{\mathrm{III}} &= \frac{m_P}{2}(\gamma w_1^{B0} + w_2^{B0})^2 + \frac{m_P}{2}(\gamma u_1^{B0} + u_2^{B0})^2 + \frac{(d_{1P} - \gamma m_P)\gamma}{2}(w_1^{B0})^2 + \frac{(d_{2P} - \gamma m_P)\gamma}{2}(u_1^{B0})^2,
\end{aligned} \tag{26}$$

and the positive constant γ is first chosen such that

$$d_{iP} - \gamma m_P \geq d_{iP}^*, i = 1, 2, \tag{27}$$

where d_{iP}^* is a strictly positive constant, and $k_{iB}, i = 1, 2, 3$ are chosen later. Note that U_1 is referred to the "energy" of the beam while it is nontrivial to choose $U_i, i = 2, 3, 4$. We now find the lower bound of U. With the use of Young's and Hölder's inequalities and the third inequality of (8) and $\sin(\theta_1) = \frac{\mathbb{D}u_1}{1+\varepsilon}$, see the second equation of (2), we can bound U_2 as:

$$\begin{aligned}
|U_2| \leq& \gamma m_0\varrho_{01}\left(\|u_2\|_{L^2}^2 + \|w_2\|_{L^2}^2\right) + \frac{\gamma m_0}{4\varrho_{01}}\left(\|u_1\|_{L^2}^2 + \|w_1\|_{L^2}^2\right) + \frac{\gamma J_0\varrho_{02}}{(1+\varepsilon_m)^2}\|\theta_2\|_{L^2}^2 + \frac{\gamma J_0\|\mathbb{D}u_1\|_{L^2}^2}{4\varrho_{02}(1+\varepsilon_m)^2}\\
\leq& \gamma m_0\varrho_{01}\left(\|w_2\|_{L^2}^2 + \|u_2\|_{L^2}^2\right) + \frac{\gamma\Gamma m_0}{2\varrho_{01}}\left[(w_1^{B\Gamma})^2 + (u_1^{B\Gamma})^2\right] + \frac{\gamma\Gamma^2 m_0}{\varrho_{01}}\left(\|\mathbb{D}w_1\|_{L^2}^2 + \|\mathbb{D}u_1\|_{L^2}^2\right)\\
&+ \frac{\gamma J_0\varrho_{02}}{(1+\varepsilon_m)^2}\|\theta_2\|_{L^2}^2 + \frac{\gamma J_0\|\mathbb{D}u_1\|_{L^2}^2}{4\varrho_{02}(1+\varepsilon_m)^2}\\
\leq& \gamma m_0\varrho_{01}\left(\|w_2\|_{L^2}^2 + \|u_2\|_{L^2}^2\right) + \frac{\gamma\Gamma m_0}{2\varrho_{01}}\left[(w_1^{B\Gamma})^2 + (u_1^{B\Gamma})^2\right] + \left(\frac{\gamma\Gamma^2 m_0}{\varrho_{01}} + \frac{\gamma J_0}{4\varrho_{02}(1+\varepsilon_m)^2}\right)\|\varepsilon\|_{L^2}^2\\
&+ 2\left(\frac{\gamma\Gamma^2 m_0}{\varrho_{01}} + \frac{\gamma J_0}{4\varrho_{02}(1+\varepsilon_m)^2}\right)\langle 1, \varepsilon - \mathbb{D}w_1\rangle_{L^2} + \frac{\gamma J_0\varrho_{02}}{(1+\varepsilon_m)^2}\|\theta_2\|_{L^2}^2
\end{aligned} \tag{28}$$

where we have used $\varepsilon^2 + 2(\varepsilon - \mathbb{D}w_1) = (\mathbb{D}w_1)^2 + (\mathbb{D}u_1)^2$, which is obtained by squaring both sides of (2) then adding together; $\varepsilon_m = \inf_{t\in[t_0,\infty)}\varepsilon(t)$, see Assumption 2.1.3; and $\varrho_{0i}, i = 1, 2$ are positive constants to be determined. Using $U_1 - |U_2| + U_3 + U_4^{\mathrm{I,II}} \leq U^{\mathrm{I,II}} \leq U_1 + |U_2| + U_3 + U_4^{\mathrm{I,II}}$ and similarly for U^{III}, and the second inequality of (8), we can bound U as follows:

$$\begin{aligned}&c_1^{\mathrm{I,II}}\mathcal{E}^{\mathrm{I,II}} \leq U^{\mathrm{I,II}} \leq \alpha_2^{\mathrm{I,II}}(\mathcal{E}^{\mathrm{I,II}}),\\ &c_1^{\mathrm{III}}\mathcal{E}^{\mathrm{III}} \leq U^{\mathrm{III}} \leq \alpha_2^{\mathrm{III}}(\mathcal{E}^{\mathrm{III}}),\end{aligned} \tag{29}$$

where $\mathcal{E}^{\mathrm{I,II}}$ and is defined in (12), $\alpha_2^{\mathrm{I,II}}$ and α_2^{III} are class $\mathcal{K}_\infty$-functions, and

$$\begin{aligned}&\text{Types I and II}: \{c_1^{\mathrm{I,II}} = c_1^{\diamond},\\ &\text{Type III}: \{c_1^{\mathrm{III}} = [c_1^{\diamond}] \wedge \Big[\frac{m_P}{2}\Big] \wedge \Big[\frac{J_P}{2}\Big] \wedge \Big[\frac{(d_{1P}-\gamma m_P)\gamma}{2}\Big] \wedge \Big[\frac{(d_{2P}-\gamma m_P)\gamma}{2}\Big],\end{aligned} \tag{30}$$

with $c_1^{\diamond}$ being defined as

$$\begin{aligned}c_1^{\diamond} =& \Big[m_0\Big(\frac{1}{2}-\gamma\varrho_{01}\Big)\Big] \wedge \Big[J_0\Big(\frac{1}{2}-\frac{\gamma\varrho_{02}}{(1+\varepsilon_m)^2}\Big)\Big] \wedge \Big[\frac{EA}{2}-\frac{\gamma\Gamma^2 m_0}{\varrho_{01}}-\frac{\gamma J_0}{4\varrho_{02}(1+\varepsilon_m)^2}\Big] \wedge \Big[\frac{EI}{2}\Big]\\ &\wedge \Big[\frac{m_{1B}}{2}\Big] \wedge \Big[\frac{m_{2B}}{2}\Big] \wedge \Big[k_{1B}\gamma-\frac{\gamma\Gamma m_0}{2\varrho_{01}}\Big] \wedge \Big[k_{2B}\gamma-\frac{\gamma\Gamma m_0}{2\varrho_{01}}\Big],\end{aligned} \tag{31}$$

and we have chosen ϱ_{01} and ϱ_{02} such that

$$P_0 \geq 2\Big(\frac{\Gamma^2 m_0}{\varrho_{01}}+\frac{J_0}{4\varrho_{02}(1+\varepsilon_m)^2}\Big) \tag{32}$$

to ensure that $\big(P_0 - 2\frac{\Gamma^2 m_0}{\varrho_{01}} - 2\frac{J_0}{4\varrho_{02}(1+\varepsilon_m)^2}\big)\big\langle 1, \varepsilon - \mathbb{D}w_1\big\rangle_{L^2} \geq 0$. The constants γ and ϱ_{01} are chosen such that

$$c_1^{\mathrm{I,II}} \geq c_1^{*\mathrm{I,II}},\ c_1^{\mathrm{III}} \geq c_1^{*\mathrm{III}}, \tag{33}$$

where $c_1^{*\mathrm{I,II}}$ and $c_1^{*\mathrm{III}}$ are strictly positive constants. This is always possible by choosing γ sufficiently small for given $\varrho_{0i}, i = 1, 2$. The constants $\varrho_{0i}, i = 1, 2$ and control gains $k_{iB}, i = 1, 2$ for a given constant axial force P_0 are chosen as in the following procedure to ensure that the conditions (27), (33), and (32) hold:

Procedure 4.1: *For a given P_0:*

Step 1. Choose $\varrho_{0i}, i = 1, 2$ such that

$$P_0 \gg 2\Big(\frac{\Gamma^2 m_0}{\varrho_{01}}+\frac{J_0}{4\varrho_{02}(1+\varepsilon_m)^2}\Big). \tag{34}$$

Step 2. Choose γ such that

$$\gamma \ll \tfrac{d_{1P}}{m_P} \wedge \tfrac{d_{2P}}{m_P} \wedge \tfrac{1}{2\varrho_{01}} \wedge \tfrac{1}{2\varrho_{02}(1+\varepsilon_m)^2} \wedge \big[\tfrac{EA}{2}\big(\tfrac{\Gamma^2 m_0}{\varrho_{01}}+\tfrac{J_0}{4\varrho_{02}(1+\varepsilon_m)^2}\big)^{-1}. \tag{35}$$

Step 3. Choose k_{iB} such that

$$k_{1B} \gg \tfrac{\Gamma m_0}{2\varrho_{01}},\quad k_{1B} \gg \tfrac{\Gamma m_0}{2\varrho_{01}}. \tag{36}$$

The symbols " $\gg$ " and " $\ll$ " mean strictly larger than, and strictly less than, respectively.

Thus, the Lyapunov functional candidate U is a proper (positive definite and radially unbounded) functional of $\mathcal{E}$. We now calculate the generators $\mathcal{L}U^{\mathrm{I,II}} := \frac{dU^{\mathrm{I,II}}}{dt}$ and $\mathcal{L}U^{\mathrm{III}} := \frac{dU^{\mathrm{III}}}{dt}$. It is obvious from (25) that

$$\begin{aligned}\mathcal{L}U^{\mathrm{I,II}} &= \mathcal{L}U_1+\mathcal{L}U_2+\mathcal{L}U_3+\mathcal{L}U_4^{\mathrm{I,II}},\\ \mathcal{L}U^{\mathrm{III}} &= \mathcal{L}U_1+\mathcal{L}U_2+\mathcal{L}U_3+\mathcal{L}U_4^{\mathrm{III}},\end{aligned} \tag{37}$$

where $\mathcal{L}U_i, i = 1, ..., 3$, $\mathcal{L}U_4^{\mathrm{I,II}}$, and $\mathcal{L}U_4^{\mathrm{III}}$ are detailed in the following subsections.

4.2.1. Calculation of $\mathcal{L}U_1$

Differentiating both sides of the first equation of (26) along the solutions of (22) results in

$$\begin{aligned}\mathcal{L}U_1 =& \big\langle \mathbb{D}[N\cos(\theta_1) - Q\sin(\theta_1) - P_0] + f_1, w_2\big\rangle_{L^2} + \big\langle \mathbb{D}[N\sin(\theta_1) + Q\cos(\theta_1)] + f_2, u_2\big\rangle_{L^2} \\ &+ \big\langle \mathbb{D}M + (1+\varepsilon)Q + f_3, \theta_2\big\rangle_{L^2} + EA\big\langle \varepsilon, \varepsilon_t\big\rangle_{L^2} + EI\big\langle \mathbb{D}\theta_1, \mathbb{D}\theta_2\big\rangle_{L^2} + P_0\big\langle 1, \varepsilon_t - \mathbb{D}w_2\big\rangle_{L^2},\end{aligned} \tag{38}$$

where $\varepsilon_t := \frac{\partial \varepsilon}{\partial t}$ and we have used the trick $\mathbb{D}[N\cos(\theta_1) - Q\sin(\theta_1)] = \mathbb{D}[N\cos(\theta_1) - Q\sin(\theta_1) - P_0]$ to deal with the boundary condition. Using integration by parts and boundary conditions (23) and (24), we can write $\mathcal{L}U_1$ as

$$\begin{aligned}\mathcal{L}U_1 =& \big\{[N^{B\Gamma}\cos(\theta_1^{B\Gamma}) - Q^{B\Gamma}\sin(\theta_1^{B\Gamma}) - P_0]w_2^{B\Gamma} + [N^{B\Gamma}\sin(\theta_1^{B\Gamma}) + Q^{B\Gamma}\cos(\theta_1^{B\Gamma})]u_2^{B\Gamma}\big\} \\ &- \big\{[N^{B0}\cos(\theta_1^{B0}) - Q^{B0}\sin(\theta_1^{B0}) - P_0]w_2^{B0} + [N^{B0}\sin(\theta_1^{B0}) + Q^{B0}\cos(\theta_1^{B0})]u_2^{B0}\big\} \\ &+ EA\big\langle \varepsilon, \varepsilon_t\big\rangle_{L^2} + EI\big\langle \mathbb{D}\theta_1, \mathbb{D}\theta_2\big\rangle_{L^2} + P_0\big\langle 1, \varepsilon_t - \mathbb{D}w_2\big\rangle_{L^2} + \Omega_1 + \big\langle f_1, w_2\big\rangle_{L^2} + \big\langle f_2, u_2\big\rangle_{L^2} + \big\langle f_3, \theta_2\big\rangle_{L^2},\end{aligned} \tag{39}$$

where

$$\begin{aligned}\Omega_1 =& -\big\langle [N\cos(\theta_1) - Q\sin(\theta_1) - P_0], \mathbb{D}w_2\big\rangle_{L^2} - \big\langle [N\sin(\theta_1) + Q\cos(\theta_1)], \mathbb{D}u_2\big\rangle_{L^2} - \big\langle M, \mathbb{D}\theta_2\big\rangle_{L^2} \\ =& -\big\langle N, [\mathbb{D}u_2\sin(\theta_1) + \mathbb{D}w_2\cos(\theta_1)]\big\rangle_{L^2} - \big\langle M, \mathbb{D}\theta_2\big\rangle_{L^2} - \big\langle Q, [\mathbb{D}\cos(\theta_1) - \mathbb{D}w_2\sin(\theta_1)]\big\rangle_{L^2} \\ &+ P_0\big\langle 1, \mathbb{D}w_2\big\rangle_{L^2}.\end{aligned} \tag{40}$$

To further calculate Ω_1, we differentiate both sides of (2) to obtain

$$\begin{aligned}\varepsilon_t &= \mathbb{D}w_2\cos(\theta_1) + \mathbb{D}u_2\sin(\theta_1), \\ 0 &= -\mathbb{D}w_2\sin(\theta_1) + \mathbb{D}u_2\cos(\theta_1) - (1+\varepsilon)\theta_2.\end{aligned} \tag{41}$$

Substituting (41) and the expression of N and M defined in (3) into (40) results in

$$\Omega_1 = -EA\big\langle \varepsilon, \varepsilon_t\big\rangle_{L^2} - EI\big\langle \mathbb{D}\theta_1, \mathbb{D}\theta_2\big\rangle_{L^2} - P_0\big\langle 1, \varepsilon_t - \mathbb{D}w_2\big\rangle_{L^2}. \tag{42}$$

Now, substituting (42) into (39) gives

$$\begin{aligned}\mathcal{L}U_1 =& \big\{[N^{B\Gamma}\cos(\theta_1^{B\Gamma}) - Q^{B\Gamma}\sin(\theta_1^{B\Gamma}) - P_0]w_2^{B\Gamma} + [N^{B\Gamma}\sin(\theta_1^{B\Gamma}) + Q^{B\Gamma}\cos(\theta_1^{B\Gamma})]u_2^{B\Gamma}\big\} \\ &- \big\{[N^{B0}\cos(\theta_1^{B0}) - Q^{B0}\sin(\theta_1^{B0}) - P_0]w_2^{B0} + [N^{B0}\sin(\theta_1^{B0}) + Q^{B0}\cos(\theta_1^{B0})]u_2^{B0}\big\} \\ &+ \big\langle f_1, w_2\big\rangle_{L^2} + \big\langle f_2, u_2\big\rangle_{L^2} + \big\langle f_3, \theta_2\big\rangle_{L^2}.\end{aligned} \tag{43}$$

4.2.2. Calculation of $\mathcal{L}U_2$

Differentiating both sides of the third equation of (26) along the solutions of (22) and using integration by parts result in

$$\begin{aligned}\mathcal{L}U_2 =& \gamma m_0\big[\|w_2\|_{L^2}^2 + \|u_2\|_{L^2}^2\big] + \Omega_{21} + \gamma\big\langle \mathbb{D}[N\cos(\theta_1) - Q\sin(\theta_1)] + f_1, w_1\big\rangle_{L^2} \\ &+ \gamma\big\langle \mathbb{D}[N\sin(\theta_1) + Q\cos(\theta_1)] + f_2, u_1\big\rangle_{L_2} + \gamma\Big\langle \mathbb{D}M + Q(1+\varepsilon) + f_3, \frac{\sin(\theta_1)}{1+\varepsilon}\Big\rangle_{L^2},\end{aligned} \tag{44}$$

with

$$\begin{aligned}\Omega_{21} =& \gamma J_0\Big\langle 1, \frac{\theta_2^2\cos(\theta_1)(1+\varepsilon) - \varepsilon_t\theta_2\sin(\theta_1)}{(1+\varepsilon)^2}\Big\rangle_{L^2} \\ \leq& \gamma J_0\Big[\frac{\varrho_{11} + \varrho_{12}}{(1+\varepsilon_m)^2} + \frac{1}{1+\varepsilon_m}\Big]\|\theta_2\|_{L^2}^2 + \frac{\gamma J_0}{4\varrho_{11}(1+\varepsilon_m)^2}\|\mathbb{D}w_2\|_{L^2}^2 + \frac{\gamma J_0}{4\varrho_{12}(1+\varepsilon_m)^2}\|\mathbb{D}u_2\|_{L^2}^2,\end{aligned} \tag{45}$$

where we have used the first equation of (41) and Young's inequality; and ϱ_{11} and ϱ_{12} are positive constants to be determined. Now, applying integration by parts to (44) and using (45) gives

$$\begin{aligned}\mathcal{L}U_2 \leq& \left\{[N^{B\Gamma}\cos(\theta_1^{B\Gamma}) - Q^{B\Gamma}\sin(\theta_1^{B\Gamma}) - P_0]\gamma w_1^{B\Gamma} + [N^{B\Gamma}\sin(\theta_1^{B\Gamma}) + Q^{B\Gamma}\cos(\theta_1^{B\Gamma})]\gamma u_1^{B\Gamma}\right\}\\ &- \left\{[N^{B0}\cos(\theta_1^{B0}) - Q^{B0}\sin(\theta_1^{B0}) - P_0]\gamma w_1^{B0} + [N^{B0}\sin(\theta_1^{B0}) + Q^{B0}\cos(\theta_1^{B0})]\gamma u_1^{B0}\right\}\\ &+ \gamma m_0\left[\|w_2\|_{L^2}^2 + \|u_2\|_{L^2}^2\right] + \gamma J_0\left[\frac{\varrho_{11}+\varrho_{12}}{(1+\varepsilon_m)^2} + \frac{1}{1+\varepsilon_m}\right]\|\theta_2\|_{L^2}^2 + \frac{\gamma J_0\|\mathbb{D}w_2\|_{L^2}^2}{4\varrho_{11}(1+\varepsilon_m)^2} + \frac{\gamma J_0\|\mathbb{D}u_2\|_{L^2}^2}{4\varrho_{12}(1+\varepsilon_m)^2}\\ &+ \gamma\left\langle Q, \sin(\theta_1)\right\rangle_{L^2} + \Omega_{22} + \Omega_{23} + \gamma\left\langle f_1, w_1\right\rangle_{L^2} + \gamma\left\langle f_2, u_1\right\rangle_{L^2} + \gamma\left\langle f_3, \frac{\sin(\theta_1)}{1+\varepsilon}\right\rangle_{L^2},\end{aligned} \tag{46}$$

where we have again used $\mathbb{D}[N\cos(\theta_1) - Q\sin(\theta_1)] = \mathbb{D}[N\cos(\theta_1) - Q\sin(\theta_1) - P_0]$, and

$$\begin{aligned}\Omega_{22} =& -\gamma\left\langle N, \cos(\theta_1)\mathbb{D}w_1 + \sin(\theta_1)\mathbb{D}u_1\right\rangle_{L^2} - \gamma\left\langle Q, -\sin(\theta_1)\mathbb{D}w_1 + \cos(\theta_1)\mathbb{D}u_1\right\rangle_{L^2} + \gamma P_0\left\langle 1, \mathbb{D}w_1\right\rangle_{L^2},\\ \Omega_{23} =& \gamma\left\langle \mathbb{D}M, \frac{\sin(\theta_1)}{1+\varepsilon}\right\rangle_{L^2}.\end{aligned} \tag{47}$$

Using (2) and the expression of N defined in (3), we can further calculate Ω_{22} as follows:

$$\begin{aligned}\Omega_{22} =& -\gamma EA\|\varepsilon\|_{L^2}^2 - \gamma\left\langle Q, \sin(\theta_1)\right\rangle_{L^2} - \gamma EA\left\langle \varepsilon, 1-\cos(\theta_1)\right\rangle_{L^2}\\ &- \gamma P_0\left\langle 1, 1-\cos(\theta_1)\right\rangle_{L^2} - \gamma P_0\left\langle 1, \varepsilon - \mathbb{D}w_1\right\rangle_{L^2}.\end{aligned} \tag{48}$$

Using the expression of M defined in (3) and integration by parts, we can further calculate Ω_{23} as follows:

$$\Omega_{23} = \gamma EI\left\langle \mathbb{D}^2\theta_1, \frac{\sin(\theta_1)}{1+\varepsilon}\right\rangle_{L^2}. \tag{49}$$

We now consider two cases:

- Case 1: If $\mathbb{D}^2\theta_1\sin(\theta_1) \leq 0$, we have

$$\begin{aligned}\Omega_{23} \leq& \frac{\gamma EI}{1+\varepsilon_M}\left\langle \mathbb{D}^2\theta_1, \sin(\theta_1)\right\rangle_{L^2}\\ =& \frac{\gamma EI}{1+\varepsilon_M}\left[M^{B\Gamma}\sin(\theta_1^{B\Gamma}) - M^{B0}\sin(\theta_1^{B0})\right] - \frac{\gamma EI}{1+\varepsilon_M}\left\langle (\mathbb{D}\theta_1)^2, \cos(\theta_1)\right\rangle_{L^2}\\ =& -\frac{\gamma EI}{1+\varepsilon_M}\left\langle (\mathbb{D}\theta_1)^2, \cos(\theta_1)\right\rangle_{L^2}\end{aligned} \tag{50}$$

  where $\varepsilon_M = \sup_{t\in[t_0,\infty)}\varepsilon(t)$, and we have used the boundary conditions (23) and (24).
- Case 2: If $\mathbb{D}^2\theta_1\sin(\theta_1) > 0$, we have

$$\begin{aligned}\Omega_{23} \leq& \frac{\gamma EI}{1+\varepsilon_m}\left\langle \mathbb{D}^2\theta_1, \sin(\theta_1)\right\rangle_{L^2}\\ =& \frac{\gamma EI}{1+\varepsilon_m}\left[M^{B\Gamma}\sin(\theta_1^{B\Gamma}) - M^{B0}\sin(\theta_1^{B0})\right] - \frac{\gamma EI}{1+\varepsilon_m}\left\langle (\mathbb{D}\theta_1)^2, \cos(\theta_1)\right\rangle_{L^2}\\ =& -\frac{\gamma EI}{1+\varepsilon_m}\left\langle (\mathbb{D}\theta_1)^2, \cos(\theta_1)\right\rangle_{L^2},\end{aligned} \tag{51}$$

  where we have used the boundary conditions (23) and (24).

Thus, the following upper-bound of Ω_{23} holds for both cases:

$$\Omega_{23} \leq -\frac{\gamma EI}{1+\varepsilon_M}\left\langle (\mathbb{D}\theta_1)^2, \cos(\theta_1)\right\rangle_{L^2} \leq -\frac{\gamma EI(1+(\mathbb{D}w_1)_m)}{(1+\varepsilon_M)^2}\|\mathbb{D}\theta_1\|_{L^2}^2, \tag{52}$$

where Assumption 2.1.3 implies that there exists a bounded $(\mathbb{D}w_1)_m := \inf_{t\in[t_0,\infty)} \mathbb{D}w_1$ and we have used $\cos(\theta_1) = \frac{1+\mathbb{D}w_1}{1+\varepsilon}$, see the second equation of (2). Substituting (48) and (52) into (46) results in

$$\begin{aligned}\mathcal{L}U_2 \leq\ & \big\{[N^{B\Gamma}\cos(\theta_1^{B\Gamma}) - Q^{B\Gamma}\sin(\theta_1^{B\Gamma}) - P_0]\gamma w_1^{B\Gamma} + [N^{B\Gamma}\sin(\theta_1^{B\Gamma}) + Q^{B\Gamma}\cos(\theta_1^{B\Gamma})]\gamma u_1^{B\Gamma}\big\} \\ & - \big\{[N^{B0}\cos(\theta_1^{B0}) - Q^{B0}\sin(\theta_1^{B0}) - P_0]\gamma w_1^{B0} + [N^{B0}\sin(\theta_1^{B0}) + Q^{B0}\cos(\theta_1^{B0})]\gamma u_1^{B0}\big\} \\ & + \gamma m_0\big[\|w_2\|_{L^2}^2 + \|u_2\|_{L^2}^2\big] + \gamma J_0\Big[\frac{\varrho_{11}+\varrho_{12}}{(1+\varepsilon_m)^2} + \frac{1}{1+\varepsilon_m}\Big]\|\theta_2\|_{L^2}^2 + \frac{\gamma J_0\|\mathbb{D}w_2\|_{L^2}^2}{4\varrho_{11}(1+\varepsilon_m)^2} + \frac{\gamma J_0\|\mathbb{D}u_2\|_{L^2}^2}{4\varrho_{12}(1+\varepsilon_m)^2} \\ & - \gamma EA\|\varepsilon\|_{L^2}^2 - \frac{\gamma EI(1+(\mathbb{D}w_1)_m)}{(1+\varepsilon_M)^2}\|\mathbb{D}\theta_1\|_{L^2}^2 - \gamma EA\big\langle\varepsilon, 1-\cos(\theta_1)\big\rangle_{L^2} - \gamma P_0\big\langle 1, 1-\cos(\theta_1)\big\rangle_{L^2} \\ & - \gamma P_0\big\langle 1, \varepsilon - \mathbb{D}w_1\big\rangle_{L^2} + \gamma\big\langle f_1, w_1\big\rangle_{L^2} + \gamma\big\langle f_2, u_1\big\rangle_{L^2} + \gamma\Big\langle f_3, \frac{\sin(\theta_1)}{1+\varepsilon}\Big\rangle_{L^2}.\end{aligned} \tag{53}$$

4.2.3. Calculation of $\mathcal{L}U_3$

Differentiating both sides of the third equation of (26) along the solutions of (23) results in

$$\begin{aligned}\mathcal{L}U_3 =\ & \big(w_2^{B\Gamma} + \gamma w_1^{B\Gamma}\big)\big[-[N^{B\Gamma}\cos(\theta_1^{B\Gamma}) - Q^{B\Gamma}\sin(\theta_1^{B\Gamma}) - P_0] + \phi_{1B} - d_{1B}w_2^{B\Gamma} \\ & - d_{1K}\mathbb{D}w_2^{B\Gamma} + f_{1B0} + m_{1B}\gamma w_2^{B\Gamma}\big] + 2k_{1B}\gamma w_1^{B\Gamma}w_2^{B\Gamma} \\ & + (u_2^{B\Gamma} + \gamma u_1^{B\Gamma})\big[-[N^{B\Gamma}\sin(\theta_1^{B\Gamma}) + Q^{B\Gamma}\cos(\theta_1^{B\Gamma})] + \phi_{2B} - d_{2B}u^{B\Gamma} - d_{2K}\mathbb{D}u_2^{B\Gamma} \\ & + f_{2B0} + m_{2B}\gamma u_2^{B\Gamma}\big] + 2k_{2B}\gamma u_1^{B\Gamma}u_2^{B\Gamma}.\end{aligned} \tag{54}$$

4.2.4. Calculation of $\mathcal{L}U_4^{I,II}$ and $\mathcal{L}U_4^{III}$

Differentiating both sides of the fourth and fifth equations of (30) along the solutions of (24) results in

$$\begin{aligned}\mathcal{L}U_4^{\mathrm{I,II}} =\ & 0, \\ \mathcal{L}U_4^{\mathrm{III}} =\ & (\gamma w_1^{B0}+w_2^{B0})\big[-(d_{1P}-m_P\gamma)w_2^{B0}+[N^{B0}\cos(\theta_1^{B0}) - Q^{B0}\cos(\theta_1^{B0}) - P_0] + d_{1K}\mathbb{D}w_2^{B0}+f_{1P0}\big] \\ & + (\gamma u_1^{B0} + u_2^{B0})\big[-(d_{2P} - m_P\gamma)u_2^{B0} + [N^{B0}\sin(\theta_1^{B0}) + Q^{B0}\cos(\theta_1^{B0})] + +d_{2K}\mathbb{D}u_2^{B0} + f_{2P0}\big] \\ & + (d_{1P} - \gamma m_P)\gamma w_1^{B0}w_2^{B0} + (d_{2P} - \gamma m_P)\gamma u_1^{B0}u_2^{B0}.\end{aligned} \tag{55}$$

Substituting (43), (53), (54), and (55) into (37) yields

$$\begin{aligned}\mathcal{L}U^{\mathrm{I,II}} &= \Omega^{B\Gamma} + \Omega_{\mathrm{I,II}}^{B0} + \Omega^{\diamond} + \Omega + \Omega_0, \\ \mathcal{L}U^{\mathrm{III}} &= \Omega^{B\Gamma} + \Omega_{\mathrm{III}}^{B0} + \Omega^{\diamond} + \Omega + \Omega_0,\end{aligned} \tag{56}$$

where

$$\begin{aligned}\Omega^{B\Gamma} =\ & \big(w_2^{B\Gamma} + \gamma w_1^{B\Gamma}\big)\big[\phi_{1B} - d_{1B}w_2^{B\Gamma} - d_{1K}\mathbb{D}w_2^{B\Gamma} + f_{1B0} + m_{1B}\gamma w_2^{B\Gamma}\big] + 2k_{1B}\gamma w_1^{B\Gamma}w_2^{B\Gamma} \\ & + (u_2^{B\Gamma} + \gamma u_1^{B\Gamma})\big[\phi_{2B} - d_{2B}u^{B\Gamma} - d_{2K}\mathbb{D}u_2^{B\Gamma} + f_{2B0} + m_{2B}\gamma u_2^{B\Gamma}\big] + 2k_{2B}\gamma u_1^{B\Gamma}u_2^{B\Gamma}, \\ \Omega_{\mathrm{I,II}}^{B0} =\ & 0, \\ \Omega_{\mathrm{III}}^{B0} =\ & (\gamma w_1^{B0} + w_2^{B0})\big[-(d_{1P} - m_P\gamma)w_2^{B0} + d_{1K}\mathbb{D}w_2^{B0} + f_{1P0}\big] + (d_{1P} - \gamma m_P)\gamma w_1^{B0}w_2^{B0} \\ & + (\gamma u_1^{B0} + u_2^{B0})\big[-(d_{2P} - m_P\gamma)u_2^{B0} + d_{2K}\mathbb{D}u_2^{B0} + f_{2P0}\big] + (d_{2P} - \gamma m_P)\gamma u_1^{B0}u_2^{B0},\end{aligned} \tag{57}$$

and

$$\begin{aligned}\Omega^{\diamond} &= \gamma m_0\big[\|w_2\|_{L^2}^2+\|u_2\|_{L^2}^2\big]+\gamma J_0\Big[\frac{\varrho_{11}+\varrho_{12}}{(1+\varepsilon_m)^2}+\frac{1}{1+\varepsilon_m}\Big]\|\theta_2\|_{L^2}^2+\frac{\gamma J_0\|\mathbb{D}w_2\|_{L^2}^2}{4\varrho_{11}(1+\varepsilon_m)^2}+\frac{\gamma J_0\|\mathbb{D}u_2\|_{L^2}^2}{4\varrho_{12}(1+\varepsilon_m)^2},\\ \Omega &= -\gamma EA\|\varepsilon\|_{L^2}^2-\frac{\gamma EI(1+(\mathbb{D}w_1)_m)}{(1+\varepsilon_M)^2}\|\mathbb{D}\theta_1\|_{L^2}^2-\gamma EA\big\langle\varepsilon,1-\cos(\theta_1)\big\rangle_{L^2}-\gamma P_0\big\langle 1,1-\cos(\theta_1)\big\rangle_{L^2}\\ &\quad-\gamma P_0\big\langle 1,\varepsilon-\mathbb{D}w_1\big\rangle_{L^2},\\ \Omega_0 &= \big\langle f_1,w_2\big\rangle_{L^2}+\big\langle f_2,u_2\big\rangle_{L^2}+\big\langle f_3,\theta_2\big\rangle_{L^2}+\gamma\big\langle f_1,w_1\big\rangle_{L^2}+\gamma\big\langle f_2,u_1\big\rangle_{L^2}+\gamma\Big\langle f_3,\frac{\sin(\theta_1)}{1+\varepsilon}\Big\rangle_{L^2}.\end{aligned} \tag{58}$$

From the expression of $\Omega^{B\Gamma}$ defined in (57), for simplicity the boundary controls $\phi_{iB}, i=1,2$ are chosen as follows

$$\begin{aligned}\phi_{1B} &= -(k_{1B}+\epsilon_{1B})\big(w_2^{B\Gamma}+\gamma w_1^{B\Gamma}\big)+d_{1B}w_2^{B\Gamma}-m_{1B}\gamma w_2^{B\Gamma},\\ \phi_{2B} &= -(k_{2B}+\epsilon_{2B})(u_2^{B\Gamma}+\gamma u_1^{B\Gamma})+d_{2B}u^{B\Gamma}-m_{2B}\gamma u_2^{B\Gamma},\end{aligned} \tag{59}$$

where the control gains k_{iB} and $\epsilon_{iB}, i=1,2$ are positive constants to be determined later. Indeed, there are many other choices of $\phi_{iB}, i=1,2$ such as output-feedback (only measurement of displacements), robust and adaptive ones, and disturbance observers. This will not be detailed here since it is widely available in control of lumped-parameter systems, see (Do & Pan, 2008b, 2009b; Y. P. Guo & Wang, 2016; Krstic et al., 1995). Substituting (59) into the expression of $\Omega^{B\Gamma}$ defined in (57) and using Young's inequality and the first two inequalities in (8) yields

$$\begin{aligned}\Omega^{B\Gamma} \leq &-k_{1B}\big(w_2^{B\Gamma}+\gamma w_1^{B\Gamma}\big)^2-d_{1K}\mathbb{D}w_2^{B\Gamma}\big(w_2^{B\Gamma}+\gamma w_1^{B\Gamma}\big)+2k_{1B}\gamma w_1^{B\Gamma}w_2^{B\Gamma}\\ &-k_{2B}(u_2^{B\Gamma}+\gamma u_1^{B\Gamma})^2-d_{2K}\mathbb{D}u_2^{B\Gamma}(u_2^{B\Gamma}+\gamma u_1^{B\Gamma})+2k_{2B}\gamma u_1^{B\Gamma}u_2^{B\Gamma}+c_0^{B\Gamma}\\ = &-k_{1B}(w_2^{B\Gamma})^2-k_{1B}\gamma(w_1^{B\Gamma})^2-k_{2B}(u_2^{B\Gamma})^2-k_{2B}\gamma(u_1^{B\Gamma})^2\\ &-d_{1K}\mathbb{D}w_2^{B\Gamma}\big(w_2^{B\Gamma}+\gamma w_1^{B\Gamma}\big)-d_{2K}\mathbb{D}u_2^{B\Gamma}(u_2^{B\Gamma}+\gamma u_1^{B\Gamma})+c_0^{B\Gamma},\end{aligned} \tag{60}$$

where

$$c_0^{B\Gamma}=\frac{1}{4\epsilon_{1B}}f_{1B0}^M+\frac{1}{4\epsilon_{2B}}f_{2B0}^M, \tag{61}$$

with $f_{iB0}^M, i=1,2$ being defined in (9). We now calculate the upper-bound of Ω_{III}^{B0}. From the expression of Ω_{III}^{B0} defined in (57), applying Young's inequality and the fourth inequality in (8) results in

$$\begin{aligned}\Omega_{\text{III}}^{B0} =&(\gamma w_1^{B0}+w_2^{B0})f_{1P0}-(d_{1P}-m_P\gamma)(w_2^{B0})^2+(\gamma u_1^{B0}+u_2^{B0})f_{2P0}-(d_{2P}-m_P\gamma)(u_2^{B0})^2\\ &+d_{1K}\mathbb{D}w_2^{B0}(\gamma w_1^{B0}+w_2^{B0})+d_{2K}\mathbb{D}u_2^{B0}(\gamma u_1^{B0}+u_2^{B0})\\ \leq&\gamma\varrho_{11}^{B0}(w_1^{B0})^2-(d_{1P}-m_P\gamma-\varrho_{12}^{B0})(w_2^{B0})^2+\gamma\varrho_{21}^{B0}(u_1^{B0})^2-(d_{2P}-m_P\gamma-\varrho_{22}^{B0})(u_2^{B0})^2\\ &+d_{1K}\mathbb{D}w_2^{B0}(\gamma w_1^{B0}+w_2^{B0})+d_{2K}\mathbb{D}u_2^{B0}(\gamma u_1^{B0}+u_2^{B0})+c_0^{B0}\\ \leq&-c_{11}^{B0}(w_1^{B0})^2+2(\gamma\varrho_{11}^{B0}+c_{11}^{B0})(w_1^{B\Gamma})^2+4(\gamma\varrho_{11}^{B0}+c_{11}^{B0})\Gamma\|\mathbb{D}w_1\|_{L^2}^2-c_{12}^{B0}(w_2^{B0})^2\\ &-c_{21}^{B0}(u_1^{B0})^2+2(\gamma\varrho_{21}^{B0}+c_{21}^{B0})(u_1^{B\Gamma})^2+4(\gamma\varrho_{21}^{B0}+c_{21}^{B0})\Gamma\|\mathbb{D}u_1\|_{L^2}^2-c_{22}^{B0}(u_2^{B0})^2\\ &+d_{1K}\mathbb{D}w_2^{B0}(\gamma w_1^{B0}+w_2^{B0})+d_{2K}\mathbb{D}u_2^{B0}(\gamma u_1^{B0}+u_2^{B0})+c_0^{B0},\end{aligned} \tag{62}$$

where we have added and subtracted $c_{11}^{B0}(w_1^{B\Gamma})^2$ and $c_{21}^{B0}(u_1^{B\Gamma})^2$ to the second inequality in (62); $c_{i1}^{B0}, i=1,2$ and $\varrho_{ij}^{B0}, (i,j)=1,2$ are positive constants to be chosen, and

$$\begin{aligned}c_{12}^{B0}&=d_{1P}-m_P\gamma-\varrho_{12}^{B0},\ c_{22}^{B0}=d_{2P}-m_P\gamma-\varrho_{22}^{B0},\\ c_0^{B0}&=\Big[\frac{\gamma}{4\varrho_{11}^{B0}}+\frac{1}{4\varrho_{12}^{B0}}\Big]f_{1P0}^M+\Big[\frac{\gamma}{4\varrho_{21}^{B0}}+\frac{1}{4\varrho_{22}^{B0}}\Big]f_{2P0}^M,\end{aligned} \tag{63}$$

where $f_{iP0}^M, i=1,2$ are defined in (9).

Next, we calculate the upper-bound of Ω defined in (58). We first consider

$$A = -\varepsilon^2 - \varepsilon(1 - \cos(\theta_1)). \tag{64}$$

From the second equation of (2), we have $\cos(\theta_1) = \frac{1+\mathbb{D}w_1}{1+\varepsilon} = \frac{\varepsilon-\mathbb{D}w_1}{1+\varepsilon}$. Using these equalities, we can calculate the term A as follows:

$$\begin{aligned} A &= -\varepsilon^2 - \varepsilon\Big(1 - \tfrac{1+\mathbb{D}w_1}{1+\varepsilon}\Big) = -\varepsilon^2 - \tfrac{\varepsilon(\varepsilon-\mathbb{D}w_1)}{1+\varepsilon}\Big) \\ &= -\varepsilon^2 - (\varepsilon - \mathbb{D}w_1) + \tfrac{\varepsilon-\mathbb{D}w_1}{1+\varepsilon} = -\varepsilon^2 - (\varepsilon - \mathbb{D}w_1) + (1 - \cos(\theta_1)) \\ &\le -\varepsilon^2 - (\varepsilon - \mathbb{D}w_1)\tfrac{1+\varepsilon_m}{1+\varepsilon} + (1 - \cos(\theta_1)) = -\varepsilon^2 - \varepsilon_m(1 - \cos(\theta_1)). \end{aligned} \tag{65}$$

With (65), we can calculate the upper-bound of Ω as follows:

$$\begin{aligned} \Omega \le &-\gamma EA\|\varepsilon\|^2_{L^2} - \frac{\gamma EI(1 + (\mathbb{D}w_1)_m)}{(1 + \varepsilon_M)^2}\|\mathbb{D}\theta_1\|^2_{L^2} - \gamma\big(P_0 + EA\varepsilon_m\big)\big\langle 1, 1 - \cos(\theta_1)\big\rangle_{L^2} \\ &- \gamma P_0\big\langle 1, \varepsilon - \mathbb{D}w_1\big\rangle_{L^2}. \end{aligned} \tag{66}$$

Now, we calculate the upper-bound of Ω_0 defined in (58). Substituting the expression of f_i defined in (4) into the expression of Ω_0 and using integration by parts, Young's inequality and the third inequality of (8), the upper-bound of Ω_0 can be calculated as

$$\begin{aligned} \Omega_0 = &- d_1\|w_2\|^2_{L^2} - d_2\|u_2\|^2_{L^2} + d_{1K}\big\langle w_2, \mathbb{D}^2 w_2\big\rangle_{L^2} + d_{2K}\big\langle u_2, \mathbb{D}^2 u_2\big\rangle_{L^2} - d_3\|\theta_2\|^2_{L^2} \\ &- \gamma d_1\big\langle w_1, w_2\big\rangle_{L^2} - \gamma d_2\big\langle u_1, u_2\big\rangle_{L^2} + \gamma d_{1K}\big\langle w_1, \mathbb{D}^2 w_2\big\rangle_{L^2} + \gamma d_{2K}\big\langle u_1, \mathbb{D}^2 u_2\big\rangle_{L^2} \\ &+ \big\langle w_2, f_{10}\big\rangle_{L^2} + \big\langle u_2, f_{20}\big\rangle_{L^2} + \big\langle \theta_2, f_{30}\big\rangle_{L^2} + \gamma\big\langle w_1, f_{10}\big\rangle_{L^2} + \gamma\big\langle u_1, f_{20}\big\rangle_{L^2} + \gamma\Big\langle \frac{\sin(\theta_1)}{1+\varepsilon}, f_{30}\Big\rangle_{L^2} \\ = &\big[d_{1K}(w_2^{B\Gamma} + \gamma w_1^{B\Gamma})\mathbb{D}w_2^{B\Gamma} + d_{2K}(u_2^{B\Gamma} + \gamma u_1^{B\Gamma})\mathbb{D}u_2^{B\Gamma}\big] - d_1\|w_2\|^2_{L^2} - d_2\|u_2\|^2_{L^2} - d_3\|\theta_2\|^2_{L^2} \\ &- \big[d_{1K}(w_2^{B0} + \gamma w_1^{B0})\mathbb{D}w_2^{B0} + d_{2K}(u_2^{B0} + \gamma u_1^{B0})\mathbb{D}u_2^{B0}\big] - d_{1k}\|\mathbb{D}w_2\|^2_{L^2} - d_{2K}\|\mathbb{D}u_2\|^2_{L^2} + A_0, \end{aligned} \tag{67}$$

with

$$\begin{aligned} A_0 = &-\gamma d_{1K}\big\langle \mathbb{D}w_1, \mathbb{D}w_2\big\rangle_{L^2} - \gamma d_{2K}\big\langle \mathbb{D}u_1, \mathbb{D}u_2\big\rangle_{L^2} - \gamma d_1\big\langle w_1, w_2\big\rangle_{L^2} - \gamma d_2\big\langle u_1, u_2\big\rangle_{L^2} \\ &+ \big\langle w_2, f_{10}\big\rangle_{L^2} + \big\langle u_2, f_{20}\big\rangle_{L^2} + \big\langle \theta_2, f_{30}\big\rangle_{L^2} + \gamma\big\langle w_1, f_{10}\big\rangle_{L^2} + \gamma\big\langle u_1, f_{20}\big\rangle_{L^2} + \gamma\Big\langle \frac{\sin(\theta_1)}{1+\varepsilon}, f_{30}\Big\rangle_{L^2} \\ \le &\frac{\gamma d_{1K}}{2}\|\mathbb{D}w_1\|^2_{L^2} + \frac{\gamma d_{1K}}{2}\|\mathbb{D}w_2\|^2_{L^2} + \frac{\gamma d_{2K}}{2}\|\mathbb{D}u_1\|^2_{L^2} + \frac{\gamma d_{2K}}{2}\|\mathbb{D}u_2\|^2_{L^2} + \frac{\gamma d_1}{2}\|w_1\|^2_{L^2} \\ &+ \frac{\gamma d_1}{2}\|w_2\|^2_{L^2} + \frac{\gamma d_1}{2}\|u_1\|^2_{L^2} + \frac{\gamma d_1}{2}\|u_2\|^2_{L^2} + \epsilon_{011}\|w_2\|^2_{L^2} + \epsilon_{012}\|u_2\|^2_{L^2} + \epsilon_{013}\|\theta_2\|^2_{L^2} \\ &+ \gamma\epsilon_{021}\|w_1\|^2_{L^2} + \gamma\epsilon_{022}\|u_1\|^2_{L^2} + \gamma\epsilon_{023}\|\mathbb{D}u_1\|^2_{L^2} + c_0^{0\Gamma} \\ \le &\Big[\frac{\gamma d_1}{2} + \epsilon_{011}\Big]\|w_2\|^2_{L^2} + \Big[\frac{\gamma d_2}{2} + \epsilon_{012}\Big]\|u_2\|^2_{L^2} + \epsilon_{013}\|\theta_2\|^2_{L^2} + \Big[\frac{\gamma d_{1K}}{2} + 2\gamma\Gamma^2(d_1 + 2\epsilon_{021})\Big]\|\mathbb{D}w_1\|^2_{L^2} \\ &+ \Big[\frac{\gamma d_{2K}}{2} + 2\gamma\Gamma^2(d_2 + 2\epsilon_{022}) + \gamma\epsilon_{023}\Big]\|\mathbb{D}u_1\|^2_{L^2} + \gamma\Gamma(d_1 + 2\epsilon_{021})(w_1^{B\Gamma})^2 + \gamma\Gamma(d_2 + 2\epsilon_{022})(u_1^{B\Gamma})^2 + c_0^{0\Gamma}, \end{aligned} \tag{68}$$

where we have used $\sin(\theta_1) = \frac{\mathbb{D}u_1}{1+\varepsilon}$ $\epsilon_{0ij}, i = 1, 2, 3; j = 1, 2$ are positive constants to be determined, and

$$c_0^{0\Gamma} = \Big[\frac{1}{4\epsilon_{011}} + \frac{\gamma}{4\epsilon_{021}}\Big]f_{10}^M + \Big[\frac{1}{4\epsilon_{012}} + \frac{\gamma}{4\epsilon_{022}}\Big]f_{20}^M + \frac{1}{4\epsilon_{013}}f_{30}^M + \frac{\gamma}{4\epsilon_{023}(1 + \varepsilon_m)^2}f_{30}^M, \tag{69}$$

with $f_{i0}^M, i = 1, 2, 3$ are defined in (9). Substituting (68) into (67 yields the upper-bound of Ω_0:

$$\begin{aligned}\Omega_0 \leq & \big[d_{1K}(w_2^{B\Gamma} + \gamma w_1^{B\Gamma})\mathbb{D}w_2^{B\Gamma} + d_{2K}(u_2^{B\Gamma} + \gamma u_1^{B\Gamma})\mathbb{D}u_2^{B\Gamma}\big] + \gamma\Gamma(d_1 + 2\epsilon_{021})(w_1^{B\Gamma})^2 \\ & - \big[d_{1K}(w_2^{B0} + \gamma w_1^{B0})\mathbb{D}w_2^{B0} + d_{2K}(u_2^{B0} + \gamma u_1^{B0})\mathbb{D}u_2^{B0}\big] + \gamma\Gamma(d_2 + 2\epsilon_{022})(u_1^{B\Gamma})^2, \\ & - \Big[d_1 - \frac{\gamma d_1}{2} - \epsilon_{011}\Big]\|w_2\|_{L^2}^2 - \Big[d_2 - \frac{\gamma d_2}{2} - \epsilon_{012}\Big]\|u_2\|_{L^2}^2 - (d_3 - \epsilon_{013})\|\theta_2\|_{L^2}^2 \\ & - d_{1K}\|\mathbb{D}w_2\|_{L^2}^2 - d_{2K}\|\mathbb{D}u_2\|_{L^2}^2 + \Big[\frac{\gamma d_{1K}}{2} + 2\gamma\Gamma^2(d_1 + 2\epsilon_{021})\Big]\|\mathbb{D}w_1\|_{L^2}^2 \\ & + \Big[\frac{\gamma d_{2K}}{2} + 2\gamma\Gamma^2(d_2 + 2\epsilon_{022}) + \gamma\epsilon_{023}\Big]\|\mathbb{D}u_1\|_{L^2}^2 + c_0^{0\Gamma}.\end{aligned} \tag{70}$$

Substituting $\Omega^\diamond$ defined in (58), (60), (66), (70), and $\Omega_{\text{I,II}}^{B0} = 0$ into (56) results in the generator $\mathcal{L}U^{\text{I,II}}$ for Types I and II of boundary conditions of the lower-end with a note that $w_1^{B0} = u_1^{B0} = 0$, see (24), which implies that $w_2^{B0} = u_2^{B0} = 0$, as follows:

$$\begin{aligned}\mathcal{L}U^{\text{I,II}} \leq & - c_{11}^{B\Gamma}(w_1^{B\Gamma})^2 - c_{12}^{B\Gamma}(w_2^{B\Gamma})^2 - c_{21}^{B\Gamma}(u_1^{B\Gamma})^2 - c_{22}^{B\Gamma}(u_2^{B\Gamma})^2 - c_{11}\|\varepsilon\|_{L^2}^2 - c_{12}\|\mathbb{D}\theta_1\|_{L^2}^2 \\ & - c_{13}\langle 1, 1 - \cos(\theta_1)\rangle_{L^2} - c_{14}\langle 1, \varepsilon - \mathbb{D}w_1\rangle_{L^2} - c_{21}\|w_2\|_{L^2}^2 - c_{22}\|u_2\|_{L^2}^2 - c_{23}\|\theta_2\|_{L^2}^2 \\ & - c_{31}\|\mathbb{D}w_2\|_{L^2}^2 - c_{32}\|\mathbb{D}u_2\|_{L^2}^2 + c_{0\Gamma} + c_0^{B\Gamma},\end{aligned} \tag{71}$$

where we have used $\varepsilon^2 = (\mathbb{D}w_1)^2 + (\mathbb{D}u_1)^2 - 2(\varepsilon - \mathbb{D}w_1)$, and

$$\begin{aligned}& c_{11}^{B\Gamma} = \gamma\big[k_{1B} - \Gamma(d_1 + 2\epsilon_{021})\big],\ c_{12}^{B\Gamma} = k_{1B},\ c_{21}^{B\Gamma} = \gamma\big[k_{2B} - \Gamma(d_2 + 2\epsilon_{022})\big],\ c_{22}^{B\Gamma} = k_{2B}, \\ & c_{11} = \gamma\Big[EA - \Big(\frac{d_{1K}}{2} + 2\Gamma^2(d_1 + 2\epsilon_{021})\Big) \vee \Big(\frac{d_{2K}}{2} + 2\Gamma^2(d_2 + 2\epsilon_{022}) + \gamma\epsilon_{023}\Big)\Big], c_{12} = \frac{\gamma EI(1 + (\mathbb{D}w_1)_m)}{(1 + \varepsilon_M)^2}, \\ & c_{13} = \gamma\big(P_0 + EA\varepsilon_m\big),\ c_{14} = \gamma\Big[P_0 - 2\Big(\frac{d_{1K}}{2} + 2\Gamma^2(d_1 + 2\epsilon_{021})\Big) \vee \Big(\frac{d_{2K}}{2} + 2\Gamma^2(d_2 + 2\epsilon_{022}) + \gamma\epsilon_{023}\Big)\Big], \\ & c_{21} = d_1 - \frac{\gamma d_1}{2} - \epsilon_{011} - \gamma m_0,\ c_{22} = d_2 - \frac{\gamma d_2}{2} - \epsilon_{012} - \gamma m_0,\ c_{23} = d_3 - \epsilon_{013} - \gamma J_0\Big(\frac{\varrho_{11} + \varrho_{12}}{(1 + \varepsilon_m)^2} + \frac{1}{1 + \varepsilon_m}\Big), \\ & c_{31} = d_{1K} - \frac{\gamma J_0}{4\varrho_{11}(1 + \varepsilon_m)^2},\ c_{32} = d_{2K} - \frac{\gamma J_0}{4\varrho_{12}(1 + \varepsilon_m)^2}.\end{aligned} \tag{72}$$

We choose the constants γ, P_0, k_{1B}, k_{2B}, $\epsilon_{0ij}, i = 1, 2, 3; j = 1, 2$, ϱ_{11}, and ϱ_{12} such that

$$\begin{aligned}& c_{ij}^{B\Gamma} > 0, (i, j) = 1, 2;\ c_{11} > 0;\ c_{12} > 0;\ c_{13} \geq 0;\ c_{14} \geq 0; \\ & c_{2i} > 0, i = 1, 2, 3; c_{31} > 0;\ c_{32} > 0.\end{aligned} \tag{73}$$

A careful look at (72) shows that there always exist the constants γ, P_0, k_{1B}, k_{2B}, $\epsilon_{0ij}, i = 1, 2, 3; j = 1, 2$, ϱ_{11}, and ϱ_{12} such that the conditions specified in (73) hold provided that the constant axial force P_0 is sufficiently large to ensure that $c_{13} \geq 0$ and $c_{14} \geq 0$. The above constants are chosen as in the following procedure to ensure that the conditions listed in (73) hold:

Procedure 4.2:

Step 1. Choose $\epsilon_{021}, \epsilon_{022}, \epsilon_{023}$ and γ such that

$$EA \gg \Big(\frac{d_{1K}}{2} + 2\Gamma^2(d_1 + 2\epsilon_{021})\Big) \vee \Big(\frac{d_{2K}}{2} + 2\Gamma^2(d_2 + 2\epsilon_{022}) + \gamma\epsilon_{023}\Big), \tag{74}$$

which is always possible under the condition (10). This step gives the first range of γ in this procedure.

Step 2. Choose k_{1B} and k_{2B} such that

$$k_{1B} \gg \Gamma(d_1 + 2\epsilon_{021}), \quad k_{2B} \gg \Gamma(d_2 + 2\epsilon_{022}). \tag{75}$$

Step 3. Choose $\epsilon_{011}, \epsilon_{012}, \epsilon_{013}$, and γ such that

$$\begin{aligned} &d_1 \gg \tfrac{\gamma d_1}{2} - \epsilon_{011} - \gamma m_0, \\ &d_2 \gg \tfrac{\gamma d_2}{2} - \epsilon_{012} - \gamma m_0, \\ &d_3 \gg \epsilon_{013} - \gamma J_0\Big(\tfrac{\varrho_{11}+\varrho_{12}}{(1+\varepsilon_m)^2} + \tfrac{1}{1+\varepsilon_m}\Big). \end{aligned} \tag{76}$$

This step gives the second range of γ in this procedure.

Step 4. Choose $\varrho_{11}, \varrho_{12}$, and γ such that

$$d_{1K} \gg \tfrac{\gamma J_0}{4\varrho_{11}(1+\varepsilon_m)^2},\ d_{2K} \gg \tfrac{\gamma J_0}{4\varrho_{12}(1+\varepsilon_m)^2}. \tag{77}$$

This step gives the third range of γ in this procedure.

The desired range of γ is the smallest one of all the above steps and the one in Procedure 4.1.

Then, there exists a positive constant c_3 such that

$$\mathcal{L}U^{\mathrm{I,II}} \leq -c_3\mathcal{E}^{\mathrm{I,II}} + c_{0\Gamma} + c_0^{B\Gamma}. \tag{78}$$

On the other hand, substituting $\Omega^\diamond$ defined in (58), (60), (66), (70), and the upper-bound of $\Omega_{\mathrm{III}}^{B0}$ defined in (62) into (56) results in the generator $\mathcal{L}U^{\mathrm{III}}$ for Type III of boundary conditions of the lower-end as follows:

$$\begin{aligned} \mathcal{L}U^{\mathrm{III}} \leq & -\bar{c}_{11}^{B\Gamma}(w_1^{B\Gamma})^2 - \bar{c}_{12}^{B\Gamma}(w_2^{B\Gamma})^2 - \bar{c}_{21}^{B\Gamma}(u_1^{B\Gamma})^2 - \bar{c}_{22}^{B\Gamma}(u_2^{B\Gamma})^2 - \bar{c}_{11}^{B0}(w_1^{B0})^2 - \bar{c}_{12}^{B0}(w_2^{B0})^2 \\ & -\bar{c}_{21}^{B0}(u_1^{B0})^2 - \bar{c}_{22}^{B0}(u_2^{B0})^2 - \bar{c}_{11}\|\varepsilon\|_{L^2}^2 - \bar{c}_{12}\|\mathbb{D}\theta_1\|_{L^2}^2 - \bar{c}_{13}\big\langle 1, 1-\cos(\theta_1)\big\rangle_{L^2} \\ -\bar{c}_{14}\big\langle 1, \varepsilon - \mathbb{D}w_1\big\rangle_{L^2} & - \bar{c}_{21}\|w_2\|_{L^2}^2 - \bar{c}_{22}\|u_2\|_{L^2}^2 - \bar{c}_{23}\|\theta_2\|_{L^2}^2 - \bar{c}_{31}\|\mathbb{D}w_2\|_{L^2}^2 - \bar{c}_{32}\|\mathbb{D}u_2\|_{L^2}^2 \\ & +c_{0\Gamma} + c_0^{B\Gamma} + c_0^{B0}, \end{aligned} \tag{79}$$

where

$$\begin{aligned} &\bar{c}_{11}^{B\Gamma} = c_{11}^{B\Gamma} - 2(\gamma\varrho_{11}^{B0} + c_{11}^{B0}),\ \bar{c}_{12}^{B\Gamma} = c_{11}^{B\Gamma},\ \bar{c}_{21}^{B\Gamma} = c_{21}^{B\Gamma} - 2(\gamma\varrho_{21}^{B0} + c_{21}^{B0}),\ \bar{c}_{22}^{B\Gamma} = c_{22}^{B\Gamma},\ \bar{c}_{11}^{B0} = c_{11}^{B0}, \\ &\bar{c}_{12}^{B0} = c_{12}^{B0},\ \bar{c}_{21}^{B0} = c_{21}^{B0},\ \bar{c}_{22}^{B0} = c_{22}^{B0}, \\ &\bar{c}_{11} = c_{11} - 4\Gamma\big[(\gamma\varrho_{11}^{B0} + c_{11}^{B0}) \vee (\gamma\varrho_{21}^{B0} + c_{21}^{B0})\big],\ \bar{c}_{12} = c_{12},\ \bar{c}_{13} = c_{13}, \\ &\bar{c}_{14} = c_{14} - 8\Gamma\big[(\gamma\varrho_{11}^{B0} + c_{11}^{B0}) \vee (\gamma\varrho_{21}^{B0} + c_{21}^{B0})\big], \\ &\bar{c}_{21} = c_{21},\ \bar{c}_{22} = c_{22},\ \bar{c}_{23} = c_{23},\ \bar{c}_{31} = c_{31},\ \bar{c}_{32} = c_{32}. \end{aligned} \tag{80}$$

We choose the constants γ, P_0, k_{1B}, k_{2B}, $\epsilon_{0ij}, i = 1,2,3; j = 1,2$, ϱ_{11}, ϱ_{12}, $c_{ij}^{B0}, (i,j) = 1,2$, ϱ_{11}^{B0}, and ϱ_{21}^{B0} such that

$$\begin{aligned} &\bar{c}_{ij}^{B\Gamma} > 0, (i,j) = 1,2; \bar{c}_{ij}^{B0} > 0, (i,j) = 1,2;\ \bar{c}_{11} > 0;\ \bar{c}_{12} > 0;\ \bar{c}_{13} \geq 0;\ \bar{c}_{14} \geq 0; \\ &\bar{c}_{2i} > 0, i = 1,2,3; \bar{c}_{31} > 0;\ \bar{c}_{32} > 0. \end{aligned} \tag{81}$$

A careful look at (72) shows that there always exist the constants γ, P_0, k_{1B}, k_{2B}, $\epsilon_{0ij}, i = 1,2,3; j = 1,2$, ϱ_{11}, ϱ_{12}, $c_{ij}^{B0}, (i,j) = 1,2$, ϱ_{11}^{B0}, and ϱ_{21}^{B0} such that the conditions specified in (81) hold provided that the constant axial force P_0 is sufficiently large to ensure that $\bar{c}_{13} \geq 0$ and $\bar{c}_{14} \geq 0$. The above constants are chosen as in the following procedure to ensure that the conditions listed in (81) hold:

Procedure 4.3: *Given γ that is chosen in Procedure 4.2, choose $\varrho_{11}^{B0}, \varrho_{21}^{B0}$, c_{11}^{B0}, and c_{21}^{B0} such that*

$$\begin{aligned} &c_{11}^{B\Gamma} \gg 2(\gamma\varrho_{11}^{B0} + c_{11}^{B0}), \\ &c_{21}^{B\Gamma} \gg 2(\gamma\varrho_{21}^{B0} + c_{21}^{B0}), \\ &c_{11} \gg 4\Gamma\big[(\gamma\varrho_{11}^{B0} + c_{11}^{B0}) \vee (\gamma\varrho_{21}^{B0} + c_{21}^{B0})\big], \\ &c_{14} \gg 8\Gamma\big[(\gamma\varrho_{11}^{B0} + c_{11}^{B0}) \vee (\gamma\varrho_{21}^{B0} + c_{21}^{B0})\big]. \end{aligned} \tag{82}$$

This choice is always possible because Procedure 4.2 ensures that $c_{11}^{B\Gamma}$, $c_{21}^{B\Gamma}$, c_{11}, and c_{14} are strictly positive.

Then, there exists a positive constant $\bar{c}_3$, which is smaller that c_3 for Types I and II of the boundary conditions at the lower end by examining (72) and (80), such that

$$\mathcal{L}U^{\text{III}} \leq -\bar{c}_3\mathcal{E}^{\text{III}} + c_{0\Gamma} + c_0^{B\Gamma} + c_0^{B0}. \tag{83}$$

It is important to observe that $\bar{c}_3$ in (83) is smaller than c_3 in (78), and there is an additional constant c_0^{B0} in (83) in comparison with (78). This is elaborating as follows. Type III of the boundary conditions at the lower-end moves freely and the payload is subject to disturbances $f_{1B0}(t)$ and $f_{2B0}(t)$. More importantly, the control forces ϕ_{1B} and ϕ_{2B} need to propagate from the top-end to the lower-end to suppress motion of the payload. It should also be noted that the aforementioned constants chosen for Type III are indeed valid for Types I and II. However, depending on a particular application, these constants should be chosen according to the specified type of boundary conditions to reduce conservation.

Remark 2: *In the case where P_0 is not sufficiently large, i.e., beams with a low tension are considered, we proceed as follows.*

- *For Types I and II, let us define*

$$\Omega_{I,II} = -c_{13}\big\langle 1, 1-\cos(\theta_1)\big\rangle_{L^2} - c_{14}\big\langle 1, \varepsilon - \mathbb{D}w_1\big\rangle_{L^2}. \tag{84}$$

Supposing that P_0 is small, then there exists nonnegative constants c_{13}^* and c_{14}^* such that

$$\begin{aligned}\Omega_{I,II} &\leq c_{13}^*\big\langle 1, 1-\cos(\theta_1)\big\rangle_{L^2} + c_{14}^*\big\langle 1, \varepsilon - \mathbb{D}w_1\big\rangle_{L^2}\\ &= c_{13}^*\big\langle 1, 1-\cos(\theta_1)\big\rangle_{L^2} + c_{14}^*\big\langle 1+\varepsilon, 1-\cos(\theta_1)\big\rangle_{L^2}\\ &\leq (c_{13}^* + c_{14}^*(1+\varepsilon_M))\big\langle 1, 1-\cos(\theta_1)\big\rangle_{L^2}\\ &\leq \Gamma(c_{13}^* + c_{14}^*(1+\varepsilon_M)),\end{aligned} \tag{85}$$

where we have used $\theta_1 \in (-\frac{\pi}{2}, \frac{\pi}{2})$ and $1-\cos(\theta_1) = 1 - \frac{1+\mathbb{D}w_1}{1+\varepsilon}$, i.e., $\varepsilon - \mathbb{D} = (1+\varepsilon)(1-\cos(\theta_1))$, and $\varepsilon_M = \sup_{t\in[t_0,\infty)}\varepsilon(t)$. With the use (85), we can write (71) as follows:

$$\mathcal{L}U^{I,II} \leq -c_3\mathcal{E}^{I,II} + c_{0\Gamma} + c_0^{B\Gamma} + \Gamma(c_{13}^* + c_{14}^*(1+\varepsilon_M)). \tag{86}$$

Note that there is an additional constant $\Gamma(c_{13}^* + c_{14}^*(1+\varepsilon_M))$ in (86) in comparison with (78). This is not surprising since a larger P_0 provides a larger axial stiffness.

- *For Type III, we carry out analysis in the same way as for Types I and II. Let us define*

$$\Omega_{III} = -\bar{c}_{13}\big\langle 1, 1-\cos(\theta_1)\big\rangle_{L^2} - \bar{c}_{14}\big\langle 1, \varepsilon - \mathbb{D}w_1\big\rangle_{L^2}. \tag{87}$$

Supposing that P_0 is small, then there exists nonnegative constants $\bar{c}_{13}^*$ and $\bar{c}_{14}^*$ such that (but using the same arguments to obtain (85)

$$\begin{aligned}\Omega_{III} &\leq \bar{c}_{13}^*\big\langle 1, 1-\cos(\theta_1)\big\rangle_{L^2} + \bar{c}_{14}^*\big\langle 1, \varepsilon - \mathbb{D}w_1\big\rangle_{L^2}\\ &\leq \Gamma(\bar{c}_{13}^* + \bar{c}_{14}^*(1+\varepsilon_M)).\end{aligned} \tag{88}$$

With (88), we can write (79) as follows:

$$\mathcal{L}U^{III} \leq -\bar{c}_3\mathcal{E}^{III} + c_{0\Gamma} + c_0^{B\Gamma} + c_0^{B0} + \Gamma(\bar{c}_{13}^* + \bar{c}_{14}^*(1+\varepsilon_M)). \tag{89}$$

The control design has been completed. We summarize the main results in the following theorem.

Theorem 4.1: *Under Assumption 2.1, the boundary controls $\phi_{iB}, i = 1,2$ given in (59) solves Control Objective 2.1 provided that the constants γ, P_0, k_{1B}, k_{2B}, ϱ_{01}, ϱ_{02}, $\epsilon_{0ij}, i = 1,2,3; j = 1,2$, ϱ_{11}, and ϱ_{12} such that the conditions specified in (73) hold for Types I and II of the boundary conditions at the lower-end; and the constants γ, P_0, k_{1B}, k_{2B}, ϱ_{01}, ϱ_{02}, $\epsilon_{0ij}, i = 1,2,3; j = 1,2$, ϱ_{11}, ϱ_{12}, $c_{ij}^{B0}, (i,j) = 1,2$, ϱ_{11}^{B0}, and ϱ_{21}^{B0} such that the conditions specified in (81) hold for Type III, and the* *conditions (27), (32), and (33) hold for Types I, II, and III. The closed-loop system consisting of (22), (6), (7) and (59) is globally well-posed and practically $\mathcal{K}_\infty$-exponentially stable at the origin. The proposed controls in (59) work for either large or small constant axial force P_0 as shown in Remark 2. The small P_0 case results in smaller convergence rate and large errors in comparison with the large P_0.*

Proof. See Appendix C.

Table 1.: Parameters of the beam system

Parameter	Description	Value
Γ	Length	200m
d_o	Outer diameter	0.3m
d_{in}	Inner diameter	0.1m
m_0	Mass per unit length	493kg/m
E	Young modulus	2×10^{10}kg/m^2
ε_M	Maximum axial strain	2×10^{-3}
ε_m	Minimum axial strain	-5×10^{-4}
d_1	Axial damping coefficient	120kg/m
d_2	Transverse damping coefficient	120kg/m
d_3	Rotating damping coefficient	60Ns
d_{1K}	Axial Kelvin-Voigt damping coefficient	60Nms
d_{2K}	Transverse Kelvin-Voigt damping coefficient	60Nms
d_{1B}	Axial actuator damping coefficient	200Ns/m
d_{2B}	Transverse actuator damping coefficient	400Ns/m
d_{1P}	Axial payload damping coefficient	250Ns/m
d_{2P}	Transverse payload damping coefficient	250Ns/m
m_{1B}	Axial actuator mass	100kg
m_{2B}	Transverse actuator mass	100kg
m_P	Payload mass	5000kg

5. Simulation results

This section illustrates the effectiveness of the proposed boundary controller via some numerical simulations for Type III of the boundary conditions at the lower-end since this type is more challenging than the other two types for the beam in moving water. The beam is made from steel and has parameters, which are given in Table 1. The external loads $f_{i0}, i = 1, 2, 3$ are taken as

$$\begin{aligned} f_{10} &= C_M \cos(\theta)\frac{\varrho_w \pi d_o^2 \vartheta_{1t}(z,t)}{4} + (C_D\cos(\theta) + C_F \sin(\theta))\frac{\varrho_w d_o}{2}\sqrt{\tfrac{8}{\pi}}\sigma_1(z,t)\vartheta_1(z,t), \\ f_{20} &= C_M \cos(\theta)\frac{\varrho_w \pi d_o^2 \vartheta_{2t}(z,t)}{4} + (C_D\cos(\theta) + C_F \sin(\theta))\frac{\varrho_w d_o}{2}\sqrt{\tfrac{8}{\pi}}\sigma_2(z,t)\vartheta_2(z,t), \\ f_{30} &= C_M \frac{\varrho_w \pi d_o^2 \vartheta_{3t}(z,t)}{4} + C_D\frac{\varrho_w d_o}{2}\sqrt{\tfrac{8}{\pi}}\sigma_3(z,t)\vartheta_3(z,t), \end{aligned} \tag{90}$$

where $\varrho_w = 1025\frac{\text{kg}}{\text{m}^3}$ is the water density; $C_M = 2$ is the fluid inertia coefficient; $C_D = 1.2$ and $C_F = 0.06$ are respectively the drag coefficient of flow past a cylinder and the skin-friction drag coefficient, which are chosen to be appropriate to the typical Reynolds number for the present application; and $\sigma_i(z,t)$ is the root mean square of the water particle velocity, $\vartheta_i(z,t)$. The water particle velocities ϑ_i are (Niedzwecki & Liagre, 2003):

$$\vartheta_i(z,t) = \textstyle\sum_{j=1}^{N_i} A_{ij}\omega_{ij}\frac{\cosh(k_{ij}z)}{\sinh(k_{ij}\Gamma)}\sin(\omega_{ij}t), \tag{91}$$

where the amplitude A_{ij}, wave number k_{ij}, and frequency ω_{ij} of the wave j^{th} are given by

$$\omega_{ij} = \omega_{im} + \frac{\omega_{im}-\omega_{iM}}{N_i} j, S_{ij} = \frac{1.25}{4}\frac{\omega_{io}^4}{\omega_j^5} H_i^2 e^{-1.25\frac{\omega_{io}^4}{\omega_j^4}}, A_{ij} = \sqrt{2S_{ij}\frac{\omega_{iM}-\omega_{im}}{N_i}},\ k_{ij}\tanh(k_{ij}\Gamma) = \frac{\omega_{ij}^2}{9.8}. \quad (92)$$

In (92), the minimum and maximum wave frequencies are $\omega_{im} = 0.2\frac{\text{rand}}{\text{s}}$, $\omega_{iM} = 2.5\frac{\text{rand}}{\text{s}}$; the two-parameter Bretschneider spectrum S_{ij} is used with the significant wave height $H_i = 4m$; the modal frequency is $\omega_{io} = \frac{2\pi}{T_i}$ with $T_i = 7.8$; and $N_i = 10$. The loads f_{iB0} are equal to the value of f_{i0} evaluated at $z = \Gamma$; and f_{iP0} are equal to 10^3 times of f_{i0} evaluated at $z = 0$.

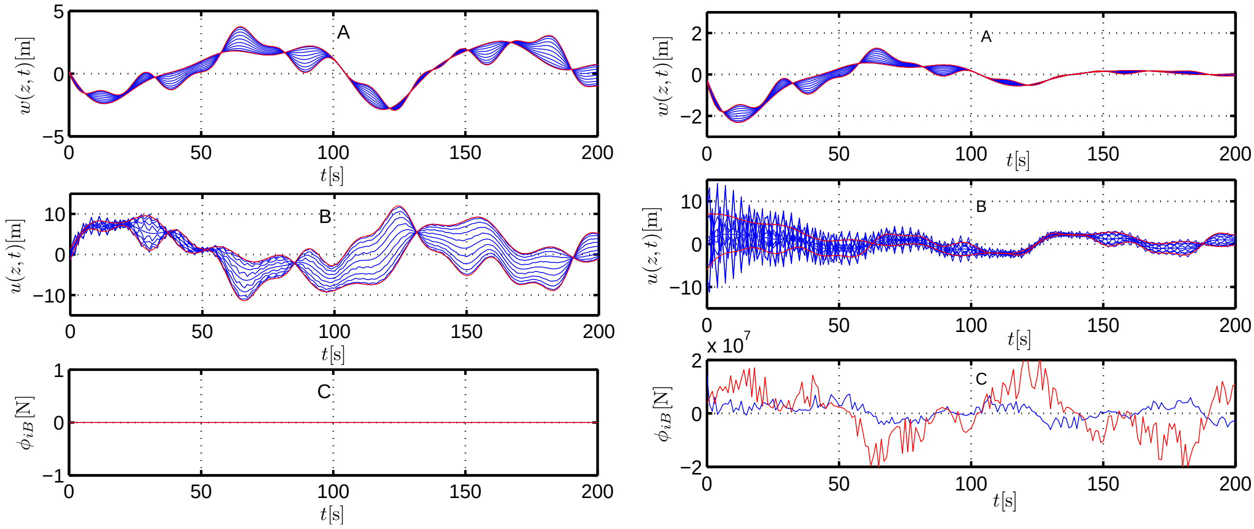

a) Simulation results without any boundary controls. b) Simulation results with boundary controls.

Figure 2.: Comparison of simulation results without and with the proposed boundary controls.

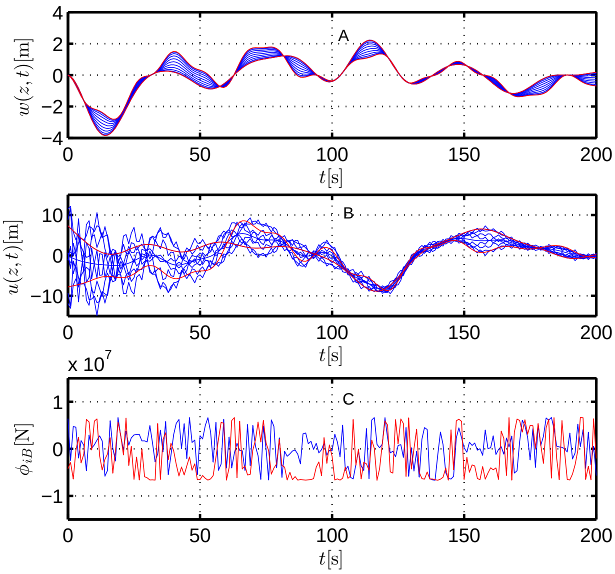

Figure 3.: Simulation results with boundary controls designed in (Do, 2017a).

Since $P_0 = m_P g < EA|\varepsilon_m|$, we are considering the small P_0 case. As per guidelines in Procedures 4.1, 4.2, 4.3, and values of the beam parameters, the control gains $k_{iB}, i = 1,2$, and γ are chosen as $k_{1B} = k_{2B} = \frac{1}{20}EA$, and $\gamma = \frac{1}{4\Gamma}$. Note that there are many other values of $k_{iB}, i = 1,2$, and γ that can be chosen according to Procedures 4.1, 4.2, 4.3. The above choice is only an example. Indeed, since $k_{iB}, i = 1,2$, and γ have been chosen according to Procedures 4.1, 4.2, 4.3, they ensure that all the conditions specified in Theorem 4.1 hold (particularly note that Remark 2 has to be applied for this case) for some positive constants $\epsilon_{0ij}, i = 1,2,3; j = 1,2$, ϱ_{11}, ϱ_{12}, $c_{ij}^{B0}, (i,j) = 1,2$, ϱ_{11}^{B0}, and ϱ_{21}^{B0}.

The initial conditions are taken as $t_0 = 0$, $w_1(t_0) = 0.2\sin\left(\frac{2\pi}{\Gamma}z\right)$, $u_1(t_0) = \cos\left(\frac{5\pi}{\Gamma}z\right)$, and $w_2(t_0) = u_2(t_0) = 0$.

The central difference scheme is used to numerically solve the partial differential equations (1) together with the boundary conditions (6), (7), where the boundary controls $\phi_{iB}, i = 1,2,3$ are given in (59). We choose the time step $\Delta t = 0.1$ and space step $\Delta s = 0.5$ to ensure that the convergence parameter $r = \frac{\Delta t}{(\Delta s)^2} = 0.4$ is positive and less than 0.5 as required for stable solutions (Smith, 1985). We run two cases: 1) without the proposed boundary controller, and 2) with the proposed boundary controller. For both cases, the length of simulation time is 200 seconds and $w(z,t)$ and $u(z,t)$ at $z = 20im, i = 0, ..., 10$ are examined.

Case 1: The results are plotted in Fig. 2a. The displacements $(w(z,t), u(z,t)$ are plotted in Sub-figs.

2a.A and 2a.B at the aforementioned locations. The red lines denote displacements of $(w(z,t), u(z,t)$ at $z = 0$ and $z = \Gamma$. The displacements and angle oscillate with quite large magnitudes due to the sea loads but are bounded due to structural stiffness. The controls are plotted in Sub-fig. 2a.C.

Case 2: The results are plotted in Fig.2b. Comparing Sub-figs. 2b.A and 2b.B in this case with corresponding Sub-figs. 2a.A and 2a.B in the case where no boundary controls are applied clearly shows that a significant reduction (about 15 times less) in magnitude of all displacements at all the examined locations. The controls are plotted in Sub-fig. 2a.C, where the blue line denotes ϕ_{1B} and the red line denotes ϕ_{2B}. Note that all the displacements do not exponentially converge to zero but to a ball centered at the origin due to the non-zero sea loads as stated in Theorem 4.1. Note also that transversal displacement $u(z,t)$ is much larger than longitudinal displacement for both cases. This is a normal observation in flexible beams due to their slenderness.

Next, we run a simulation with the boundary controls designed in (Do, 2017a) for comparison, see Fig. 3. The reason that the control design in (Do, 2017a) is chosen for comparison is because all the control designs, which appeared before the one in (Do, 2017a), for a linearized model of (1) are suffering from stability issue as mentioned in (Do, 2017a), Subsections 1.1 and 1.2, and Remark 4.3 (Item 3). As mentioned in Section 1, the model used in (Do, 2017a) was obtained by linearizing (1) at the origin. Thus the controls in (Do, 2017a) can only handle small motions. This can be clearly seen from Sub-figs 3.A and 3.B, the controls, which are plotted in Sub-fig. 3.C, where the small motions around the large ones reduce. It is also observed that the controls plotted in Sub-fig. 3.C contain only small signals.

6. Conclusions

A design of boundary controls was proposed to globally practically $\mathcal{K}_\infty$-exponentially stabilize large motions of Euler-Bernoulli beams with non-neglectable moment of inertia under external loads. Three types of boundary conditions were considered, where Type III is the most challenging. This is because: physically the lower-end is freely moving, and theoretically Sobolev embedding has to use to relate motion of the lower-end to that of the top-end and the controls need to propagate from the top-end to the lower-end. Future work is extend the current work to the space case for (particularly) Type III of boundary conditions at the lower-end.

Appendices

Appendix A. Proof of Lemma 2.1

To prove the first equation of (8), we note from (2) that

$$(1+\varepsilon)^2 = (1+w_z)^2 + u_z^2 \geq (1+w_z)^2, \tag{A1}$$

for all $(z,t) \in [0,\Gamma] \times [t_0, \infty)$, which gives the first inequality of (8) after a simple manipulation. To prove the second equality of (8), we note from the first equation of (A1) that

$$\varepsilon^2 = w_z^2 + u_z^2 - 2(\varepsilon - w_z), \tag{A2}$$

which gives the second inequality of (8). The third inequality follows from Lemma 3 in (Do & Pan, 2008a). To prove the fourth inequality of (8), we use Lemma 4 in (Do & Pan, 2008a) and Young's inequality to obtain

$$\begin{aligned} w^2(0,t) &\leq w^2(\Gamma,t) + 2\sqrt{\int_0^\Gamma w^2(z,t)dz}\sqrt{\int_0^\Gamma w_z^2(z,t)dz} \\ &\leq (1+2\Gamma\rho)w^2(\Gamma,t) + \left(4\rho\Gamma^2 + \frac{1}{\rho}\right)\int_0^\Gamma w_z^2(z,t)dz \end{aligned} \tag{A3}$$

where we have used the first third inequality of (8) and ρ is a positive constant, which gives the fourth inequality of (8) by picking $\rho = \frac{1}{2\Gamma}$. □

Appendix B. Proof of Theorem 3.2

Since all the conditions of Theorem 3.1 hold, the system (14) has a unique variational solution. We now calculate $U(\boldsymbol{X},t)$ as

$$U(\boldsymbol{X}(t),t) = U(\boldsymbol{X}(s),s) + \int_s^t \mathcal{L}U(\boldsymbol{X}(r),r)dr. \tag{B1}$$

Applying the conditions (20) and (21) to (B1) yields

$$c_1\|\boldsymbol{X}(t)\|_H^2 \leq \alpha_2(\|\boldsymbol{X}(s)\|_H^2) - \int_s^t \Big(c_3\|\boldsymbol{X}(r)\|_H^2 - c_0\Big)dr. \tag{B2}$$

Applying the Gronwall inequality shows that there exists $\delta := \delta(\|\boldsymbol{X}_0\|_H)$ such that

$$\sup_{t_0\leq s\leq t} \|\boldsymbol{X}(s)\|_H \leq \delta(\|\boldsymbol{X}(t_0)\|_H) \tag{B3}$$

for each $\boldsymbol{X}_0 \in H$ and a.e. $(t, \boldsymbol{X}(t) \in [t_0,\infty) \times V$. This proves global stability of (14). Let us define $c_2 = \frac{\alpha_2(\|\boldsymbol{X}_0\|_H^2)}{\|\boldsymbol{X}_0\|_H^2}$, which is well-defined and is a non-decreasing function of $\|\boldsymbol{X}_0\|_H^2$ because α_2 is a class $\mathcal{K}_\infty$-function. Now, we calculate $e^{\frac{c_3}{c_2}(t-t_0)}U(\boldsymbol{X}(t),t)$ along the solutions of (14) as

$$e^{\frac{c_3}{c_2}(t-t_0)}U(\boldsymbol{X}(t),t) = U(\boldsymbol{X}(t_0),t_0) + \int_{t_0}^t e^{\frac{c_3}{c_2}(\tau-t_0)}\Big(\mathcal{L}U(\boldsymbol{X}(\tau),\tau) + \frac{c_3}{c_2}U(\boldsymbol{X}(\tau),\tau)\Big)d\tau. \tag{B4}$$

Applying the conditions (20) and (21) to (B4) and using (B3) yield

$$\begin{aligned}
e^{\frac{c_3}{c_2}(t-t_0)}c_1\|\boldsymbol{X}(t)\|_H^2 &\leq \alpha_2(\|\boldsymbol{X}_0\|_H^2) + \int_{t_0}^t e^{\frac{c_3}{c_2}(\tau-t_0)}\Big(-c_3\|\boldsymbol{X}(\tau)\|_H^2 + c_0 + \frac{c_3}{c_2}\alpha_2(\|\boldsymbol{X}(\tau)\|_H^2)\Big)d\tau \\
&\leq \alpha_2(\|\boldsymbol{X}_0\|_H^2) + \int_{t_0}^t e^{\frac{c_3}{c_2}(\tau-t_0)}\Big(-c_3\|\boldsymbol{X}(\tau)\|_H^2 + c_0 + \frac{c_3}{c_2}\frac{\alpha_2(\|\boldsymbol{X}_0\|_H^2)}{\|\boldsymbol{X}_0\|_H^2}\|\boldsymbol{X}(\tau)\|_H^2\Big)d\tau \\
&= \alpha_2(\|\boldsymbol{X}_0\|_H^2) + \int_{t_0}^t e^{\frac{c_3}{c_2}(\tau-t_0)}c_0 d\tau,
\end{aligned} \tag{B5}$$

which by applying the Gronwall inequality further yields the proof of Theorem 3.2. □

Appendix C. Proof of Theorem 4.1

We only provide proof of Theorem 4.1 for Type III of the boundary conditions at the lower-end. The proof for Types I and II can be carried out similarly. Let us define $\boldsymbol{X} = \mathrm{col}(w_1, u_1, \theta_1, w_2, u_2, \theta_2, w_1^{B\Gamma}, u_1^{B\Gamma}, w_2^{B\Gamma}, u_2^{B\Gamma}, w_1^{B0}, u_1^{B0}, w_2^{B0}, u_2^{B0})$ and $\boldsymbol{F}(X,t) = \mathrm{col}(w_2, u_2, \theta_2, F_1, F_2, F_3, w_2^{B\Gamma}, u_2^{B\Gamma}, F_1^{B\Gamma}, F_2^{B\Gamma}, w_2^{B0}, u_2^{B0}, F_1^{B}, F_2^{B0})$, where $F_i, i = 1,2,3$; $F_i^{B\Gamma}, i = 1,2$; and $F_i^{B0}, i = 1,2$ are defined in (22), (23), and (24) with $\phi_{iB}, i = 1,2$ being defined in (59), respectively. Then, we can write (22), (23), and (24) as (14). Thus, to study well-posedness and stability of the closed-loop system together with the static boundary conditions in (23) and (24), we introduce the functional spaces: $H = (W^{1,2}(\mathcal{D}))^3 \times (L^2(\mathcal{D}))^3 \times \mathbb{R}^8$, $V = (W_0^{1,2}(\mathcal{D}))^3 \times (L_0^2(\mathcal{D}))^3 \times \mathbb{R}^8$, $V^* = (W^{-1,2}(\mathcal{D}))^3 \times (L^2(\mathcal{D}))^3 \times \mathbb{R}^8$, where $\mathcal{D} := (0,\Gamma)$, $W^{-m,p}(\mathcal{D})$ denotes the dual of $W^{m,p}(\mathcal{D})$; $W_0^{1,2}(\mathcal{D})$ and $L_0^2(\mathcal{D})$ denotes $W^{1,2}$- and L^2-spaces satisfying the static boundary conditions in (23) and (24). Then, we have the embedding $V \subset H \equiv H^* \subset V^*$. Let

$\boldsymbol{X} = \text{col}(\bar{w}_1, \bar{u}_1, \bar{\theta}_1, \bar{w}_2, \bar{u}_2, \bar{\theta}_2, \bar{w}_1^{B\Gamma}, \bar{u}_1^{B\Gamma}, \bar{w}_2^{B\Gamma}, \bar{u}_2^{B\Gamma}, \bar{w}_1^{B0}, \bar{u}_1^{B0}, \bar{w}_2^{B0}, \bar{u}_2^{B0})$. Define

$$\begin{aligned}\langle \boldsymbol{X}, \bar{\boldsymbol{X}} \rangle_H = & \frac{m_0}{2}\left[\langle w_2, \bar{w}_2 \rangle_{L^2} + \langle u_2, \bar{u}_2 \rangle_{L^2}\right] + \frac{J_0}{2}\langle \theta_2, \bar{\theta}_2 \rangle_{L^2} + \frac{EA}{2}\langle \varepsilon, \bar{\varepsilon} \rangle_{L^2} + \frac{EI}{2}\langle \mathbb{D}\theta_1, \mathbb{D}\bar{\theta}_1 \rangle_{L^2} \\ & + \frac{P_0}{2}\langle 1, \varepsilon - \mathbb{D}w_1 \rangle_{L^2} + \frac{P_0}{2}\langle 1, \bar{\varepsilon} - \mathbb{D}\bar{w}_1 \rangle_{L^2} + \frac{\gamma m_0}{2}\langle w_1, \bar{w}_2 \rangle_{L^2} + \frac{\gamma m_0}{2}\langle \bar{w}_1, w_2 \rangle_{L^2} \\ & + \frac{\gamma m_0}{2}\langle u_1, \bar{u}_2 \rangle_{L^2} + \frac{\gamma m_0}{2}\langle \bar{u}_1, u_2 \rangle_{L^2} + \frac{\gamma J_0}{2}\left\langle \theta_2, \frac{\sin(\bar{\theta}_1)}{1+\bar{\varepsilon}} \right\rangle_{L^2} + \frac{\gamma J_0}{2}\left\langle \bar{\theta}_2, \frac{\sin(\theta_1)}{1+\varepsilon} \right\rangle_{L^2} \\ & + \frac{m_{1B}}{2}\left(w_2^{B\Gamma} + \gamma w_1^{B\Gamma}\right)\left(\bar{w}_2^{B\Gamma} + \gamma \bar{w}_1^{B\Gamma}\right) + \frac{m_{2B}}{2}\left(u_2^{B\Gamma} + \gamma u_1^{B\Gamma}\right)\left(\bar{u}_2^{B\Gamma} + \gamma \bar{u}_1^{B\Gamma}\right) \\ & + k_{1B}\gamma w_1^{B\Gamma}\bar{w}_1^{B\Gamma} + k_{2B}\gamma u_1^{B\Gamma}\bar{u}_1^{B\Gamma} + \frac{m_P}{2}(\gamma w_1^{B0} + w_2^{B0})(\gamma \bar{w}_1^{B0} + \bar{w}_2^{B0}) + \frac{m_P}{2}(\gamma u_1^{B0} \\ & + u_2^{B0})(\gamma \bar{u}_1^{B0} + \bar{u}_2^{B0}) + \frac{(d_{1P} - \gamma m_P)\gamma}{2} w_1^{B0}\bar{w}_1^{B0} + \frac{(d_{2P} - \gamma m_P)\gamma}{2} u_1^{B0}\bar{u}_1^{B0}.\end{aligned} \tag{C1}$$

where $\bar{\varepsilon}$ is the value of ε with $\mathbb{D}u_1$, $\mathbb{D}w_1$, and θ_1 being replaced by $\mathbb{D}\bar{u}_1$, $\mathbb{D}\bar{w}_1$, and $\bar{\theta}_1$, respectively. The constant γ and the constant axial force P_0 satisfy the conditions specified in Theorem 4.1. Let us denote by $\langle \boldsymbol{X}, \bar{\boldsymbol{X}} \rangle_{LH}$ linearization of $\langle \boldsymbol{X}, \bar{\boldsymbol{X}} \rangle_H$ at the origin. Then, it can be verified that $\langle \boldsymbol{X}, \bar{\boldsymbol{X}} \rangle_{LH}$ is a inner product with the norm $\langle \boldsymbol{X}, \boldsymbol{X} \rangle_{LH} = \|\boldsymbol{X}\|^2_{LH}$. In fact, there exist strictly positive constants $\bar{c}_{01}$ and $\bar{c}_{02}$ such that $\bar{c}_{01}\mathcal{E}^{\text{III}}_{LH} \leq \|\boldsymbol{X}\|^2_{LH} \leq \bar{c}_{02}\mathcal{E}^{\text{III}}_{LH}$ locally, where $\mathcal{E}_{LH}$ is the linearization of $\mathcal{E}^{\text{III}}$ with $\mathcal{E}^{\text{III}}$ defined in (12), which is defined in (12).

Now, to prove Theorem 4.1 we just need to verify all the conditions of Theorem 3.2. The continuity condition in Assumption 3.1 holds due to continuity of $\boldsymbol{F}(\boldsymbol{X}, t)$. By using $\langle \boldsymbol{X} - \bar{\boldsymbol{X}}, \boldsymbol{F}(\boldsymbol{X}, t) - \boldsymbol{F}(\bar{\boldsymbol{X}}, t) \rangle_{V,V^*} = \langle \boldsymbol{X} - \bar{\boldsymbol{X}}, \boldsymbol{F}(\boldsymbol{X}, t) - \boldsymbol{F}(\bar{\boldsymbol{X}}, t) \rangle_H$ with the use of the local inner product in LH defined as above and integration by parts similarly to the calculation of $\mathcal{L}U$ in Section 4, it is readily shown that the local monotonicity condition (16) holds. From the second inequality of (29) and (83), it is clear that the conditions (20) and (21) hold. Thus, proof of Theorem 4.1 is completed. □

References

Adams, R. A., & Fournier, J. J. F. (2003). *Sobolev spaces* (2nd ed.). Oxford, UK: Academic Press.

Athisakul, C., Monprapussorn, T., & Chucheepsakul, S. (2011). A variational formulation for three-dimensional analysis of extensible marine riser transporting fluid. *Ocean Engineering*, *38*, 609-620.

Banks, H. T., Smith, R. C., & Wang, Y. (1996). *Smart material structures.* Paris: John Wiley & Son.

Berrimi, S., & Messaoudi, S. A. (2004). Exponential decay of solutions to a viscoelastic equation with nonlinear localized damping. *Electronic Journal of Differential Equations*, *88*, 1-10.

Bohm, M., Krstic, M., Kuchler, S., & Sawodny, O. (2014). Modelling and boundary control of a hanging rope immersed in water. *Journal of Dynamic Systems, Measurement, and Control*, *136*, 011006-1:011006-15.

Cavalcanti, M. M., Cavalcanti, V. N. D., & Soriano, J. A. (2002). Exponential decay for the solution of semilinear viscoelastic wave equations with localized damping. *Electronic Journal of Differential Equations*, *44*, 1-14.

Chen, X., Chentouf, B., & Wang, J. M. (2014). Nondissipative torque and shear force controls of a rotating fexible structure. *SIAM Journal on Control and Optimization*, *52*, 3287-3311.

Chentouf, B., & Wang, J. M. (2015). On the stabilization of the disk-beam system via torque and direct strain feedback controls. *IEEE Transactions on Automatic Control*, *60*, 3006-3011.

Chow, P. L. (2007). *Stochastic partial differential equations.* Boca Raton: Chapman & Hall/CRC.

Chow, S. T., & Sethna, P. R. (1965). Nonlinear effects of large deflections and material damping on the steady state vibrations of beams. *Tecnical Report, University of Minnesota.*

Do, K. D. (2011). Global stabilization of three-dimensional flexible marine risers by boundary control. *Ocean Systems Engineering*, *1*(2), 171-194.

Do, K. D. (2016a). Boundary control of elastic systems. *Journal of Applied Mathematics and Computing*, *51*(1), 315-339.

Do, K. D. (2016b). Stability of nonlinear stochastic distributed parameter systems and its applications. *Journal of Dynamic Systems, Measurement, and Control*, *138*, 101010-1:101010-12.

Do, K. D. (2017a). Boundary control design for extensible marine risers in three dimensional space. *Journal of Sound and Vibration*, *388*, 1-19.

Do, K. D. (2017b). Stochastic boundary control design for extensible marine risers in three dimensional space. *Automatica*, *77*, 184-197.

Do, K. D. (2017c). Stochastic boundary control design for timoshenko beams with large motions. *Journal of Sound and Vibration*, *402*, 164-184.

Do, K. D., & Pan, J. (2008a). Boundary control of transverse motion of marine risers with actuator dynamics. *Journal of Sound and Vibration*, *318*(4-5), 768-791.

Do, K. D., & Pan, J. (2008b). Nonlinear control of an active heave compensation system. *Ocean Engineering, In Press*, *35*(5-6), 558-571.

Do, K. D., & Pan, J. (2009a). Boundary control of three-dimensional inextensible marine risers. *Journal of Sound and Vibration*, *327*(3-5), 299-321.

Do, K. D., & Pan, J. (2009b). *Control of ships and underwater vehicles.* Springer.

Endo, T., Matsuno, F., & Jia, Y. (2017). Boundary cooperative control by flexible Timoshenko arms. *Automatica*, *81*, 377-389.

Eringen, A. C. (1952). On the nonlinear vibration of elastic bars. *Quarterly of Applied Mathematics*, *9*, 361-369.

Evans, L. (2000). *Partial differential equations.* Providence: American Mathematical Society.

Fard, M. P., & Sagatun, S. I. (2001). Exponential stabilization of a transversely vibrating beam by boundary control via lyapunov's direct method. *Journal of Dynamic Systems, Measurement, and Control*, *123*, 195-200.

Gawarecki, L., & Mandrekar, V. (2011). *Stochastic differential equations in infinite dimensions with applications to stochastic partial differential equations.* Berlin: Springer.

Guo, B. Z. (2001). Riesz basis approach to the stabilization of a flexible beam with a tip mass. *SIAM Journal of Control and Optimization*, *39*, 1736-1747.

Guo, B. Z., & Jin, F. F. (2013). The active disturbance rejection and sliding mode control approach to the stabilization of the Euler-Bernoulli beam equation with boundary input disturbance. *Automatica*, *49*, 2911-2918.

Guo, F., & Huang, F. (2001). Boundary feedback stabilization of the undamped euler–bernoulli beam with both ends free. *SIAM Journal of Control and Optimization*, *43*, 341-356.

Guo, Y. P., & Wang, J. M. (2016). The active disturbance rejection control of the rotating disk-beam system with boundary input disturbances. *International Journal of Control*, *89*, 2322-2335.

Harland, N. R., Mace, B. R., & Jones, R. W. (2001). Adaptive-passive control of vibration transmission in beams using electro/magnetorheological fluid filled inserts. *IEEE Transactions on Control Systems Technology*, *9*, 209-220.

He, W., Huang, T. M. D., & Li, X. (2017). Adaptive boundary iterative learning control for an Euler-Bernoulli beam system with input constraint. *IEEE Transactions on Neural Networks and Learning Systems, In Press*.

He, W., Nie, S., Meng, T., & Liu, Y. J. (2017). Modeling and vibration control for a moving beam with application in a drilling riser. *IEEE Transactions on Control Systems Technology*, *25*, 1036-1043.

Henikl, J., Kemmetmüller, W., Meurer, T., & Kugi, A. (2016). Infinite-dimensional decentralized damping control of large-scale manipulators with hydraulic actuation. *Automatica*, *63*, 101-115.

Jin, F. F., & Guo, B. Z. (2015). Lyapunov approach to output feedback stabilization for the Euler-Bernoulli beam equation with boundary input disturbance. *Automatica*, *52*, 95-102.

Kater, A., & Meurer, T. (2016). Modelling and flatness-based motion planning for an interconnected flexible beam structure. *IEEE 55th Conference on Decision and Control*, 520-525.

Khalil, H. (2002). *Nonlinear systems.* Prentice Hall.

Kokarakis, J. E., & Bernitsas, M. M. (1987). Nonlinear three-dimensional dynamic analysis of marine risers. *Journal of Energy Resources Technology*, *109*, 105-111.

Krstic, M., Kanellakopoulos, I., & Kokotovic, P. (1995). *Nonlinear and adaptive control design.* New York: Wiley.

Krstic, M., & Smyshlyaev, A. (2008). Adaptive control of PDEs. *Annual Reviews in Control*, *32*, 149-160.

Lacarbonara, W. (2013). *Nonlinear structural mechanics.* New York: Springer.

Lagnese, J. E., Leugering, G., & Schmidt, E. J. P. G. (1994). *Modeling, analysis and control of dynamic elastic multi-link structures.* Boston: Birkhäuser.

Li, Y., Xu, G., & Han, Z. (2016). Stabilization of an eulerbernoulli beam system with a tip mass subject to non-uniform bounded disturbance. *IMA Journal of Mathematical Control and Information*, 1-16.

Liu, K., & Liu, Z. (1998). Exponential decay of energy of the euler–bernoulli beam with locally distributed kelvin–voigt damping. *SIAM Journal of Control and Optimization*, *36*, 1086-1098.

Liu, K., & Liu, Z. (2000). Boundary stabilization of a nonhomogeneous beam with rotatory inertia at the tip. *Journal of Computational and Applied Mathematics*, *114*, 1-10.

Love, A. (1920). *A treatise on the mathematical theory of elasticity* (3rd ed.). Cambridge University Press.

Lu, L., Chen, Z., Yao, B., & Wang, Q. (2013). A two-loop performance oriented tip tracking control of a linear motor driven flexible beam system with experiments. *IEEE Transactions on Industrial Electronics*, *60*, 1011-1022.

Luo, Z. H., Guo, B. Z., & Morgul, O. (1999). *Stability and stabilization of infinite dimensional systems with applications.* Springer-Verlag.

Meirovitch, L. (1967). *Analytical methods in vibrations.* New York: Macmillan.

Meurer, T., Thull, D., & Kugi, A. (2008). Flatness-based tracking control of a piezoactuated Euler-Bernoulli beam with non-collocated output feedback: theory and experiments. *International Journal of Control*, *81*, 475-493.

Miletíc, M., Stürzer, D., Arnold, A., & Kugi, A. (2016). Stability of an Euler-Bernoulli beam with a nonlinear dynamic feedback system. *IEEE Transactions on Automatic Control*, *61*, 2782-2795.

Nguyen, T. L., Do, K. D., & Pan, J. (2013). Boundary control of two-dimensional marine risers with bending couplings. *Journal of Sound and Vibration*, *332*(16), 3605-3622.

Niedzwecki, J. M., & Liagre, P. Y. F. (2003). System identification of distributed-parameter marine riser models. *Ocean Engineering*, *30*(11), 1387-1415.

Özer, A. O. (2017). Modeling and controlling an active constrained layer (acl) beam actuated by two voltage sources with/without magnetic effects. *IEEE Transactions on Automatic Control, In press*.

Paranjape, A., Chung, S.-J., & Krstic, M. (2013). PDE boundary control for flexible articulated wings on a robotic aircraft. *IEEE Transactions on Robotics*, *29*, 625-640.

Queiroz, M. S. D., Dawson, M., Nagarkatti, S., & Zhang, F. (2000). *Lyapunov-based control of mechanical systems*. Boston: Birkhauser.

Smith, G. D. (1985). *Numerical solutions of partial differential equations: Finite difference methods* (3rd ed.). Oxford: Clarendon Press.